Erosion Sub-model

L.J. Hagen[*]

[*]Updated 2012, W.J. Rust. Updated 2015, F.A. Fox

Contents

List of Figures

1 Introduction

The Wind Erosion Prediction System (WEPS) is a continuous, process-based model whose purpose is to estimate wind erosion on crop lands (Hagen 1991a; USDA-ARS 2013). WEPS is composed of a user-interface, databases, and a science model composed of several sub-models. The sub-models include erosion (ESM), crop growth, residue decomposition, hydrology, soil and management. Ancillary models include weather and wind simulations. The submodels estimate the soil/vegetation "surface state" on a daily basis with respect to the erodibility of the surface. If the wind speed during the day generates an erosive force that exceeds the erodibility threshold of that surface, then the ESM will simulate the amount of wind erosion that occurs on a sub-daily time step for that day. To aid in estimating onsite and offsite impacts of erosion, the sub-model predicts the size components of the moving soil.

In addition to WEPS, a second model has been created that uses ESM. The Single Wind Erosion Event Program (SWEEP) models single day wind events. It simulates a single day from a WEPS run making possible rapid evaluations of the effect of the surface state on wind erosion potential.

1.1 Background

The dire consequences of wind erosion were dramatically demonstrated during the Dustbowl period of the United States Plains region during the 1930's. The combination of high temperatures, drought conditions and intensive tillage practices led to gigantic clouds of wind-blown soil, some of which reached great cities on the East Coast of the United States. These clouds lead to significant health problems for residents of the Dustbowl regions as well as significantly diminishing the fertility of the soil for agriculture. In response, the federal government established the Wind Erosion Research Unit (WERU) in the Department of Agriculture and charged it with doing the basic research needed to understand the wind erosion process and ways to mitigate the effects of wind erosion on the nation's farms. WEPS is part of WERU's response to that mandate.

The Natural Resources Conservation Service (NRCS) has adopted WEPS as their primary tool for evaluating management effects on wind erosion susceptibility. To facilitate serving their customers, NRCS requested a maximum WEPS run-time of one minute on fields with a crop rotation length of a single year. The stringent run-time requirement influenced many choices in developing ESM as well as other WEPS sub-models, while still maintaining the overall goal of developing a physically-based model. To reduce run-time in the ESM, quasi-steady state solutions to differential equations were used to simulate the eroding soil loss and deposition. To initiate erosion, a static threshold friction velocity of 0.23 $\frac{m}{s}$ or more was selected to skip erosion calculations during minor erosion events. A coarse mesh of rectangular grid cells was imposed upon the simulation region to allow spatial updates of the surface during erosion events, while minimizing the number of calculation cells. To confine the calculations to a single pass in each time step, the order of erosion calculation was always from upwind to downwind cells. Finally to minimize the number of time steps required, the duration of each time step was made dependent on erosion amounts. These limitations and any methods implemented for overriding them are noted in their specific sections below.

1.2 Erosion Processes

Wind erosion is the process of soil particles on the soil surface moving due to wind. Modelling the erosion of soil by wind starts as a classic fluid dynamics problem. The fluid, air, moves across a surface. The moving fluid creates a shear force on the surface. The shear force acts on loose material on the surface, and at some magnitude causes the unattached material to move, either along the surface or up into the air stream.

Undisturbed land with adequate vegetation does not erode due to wind. A lack of vegetation due to natural conditions or land management can allow wind erosion to occur, although simply working the land is not sufficient to cause wind erosion. Sandy and silty soils tend to erode more easily than does clay or rock dominated soils. Wind barriers, growing crops, crop residue, snow and rain modify erodibility. Wind barriers and growing crops reduce the effective surface shear force. Snow changes the soil surface by making it inaccesible. Crop residue, both standing and flat, does both. Moisture from rainfall adheres soil particles to the surface.

1.3 Submodel Structure

The ESM uses parameters supplied by other sub-models that describe the soil surface, flat biomass cover, standing biomass leaf and stem areas, wind barriers and weather to: a) determine if wind erosion can occur in a simulation region on a given day, b) simulate the processes of wind erosion, when erosion occurs and c) update changes in the soil surface during erosion events. Surface updating enables the model to simulate both source limited and wind energy limited erosion events. Both the surface descriptions and the simulated erosion processes were defined so that each can be experimentally measured (Hagen 2001; Mirzamostafa et al. 1998).

1.4 Submodel Outputs

The main sub-model outputs are daily estimates of both total soil loss from the simulation region as well as components of the soil loss moving across each field boundary. These components are saltation/creep (>0.10 mm diameter) and suspended soil (<0.10 mm diameter). The mass of particles less than 10 microns in aerodynamic diameter (PM_{10}) in the suspended soil are also predicted. Files of time-varying emissions from all simulation region subdivisions for use as source terms in dust diffusion and transport models can also be output. To compare simulation results to measured erosion data, input files with measured weather and measured surface conditions can be used in place of simulated weather and simulated surface conditions.

2 Operation Overview

The purpose of ESM is to estimate the amount of soil displacement in a defined field with defined surface and soil characteristics and a defined wind profile over a defined time. All of these defined parameters implicitly make assumptions that need to be carefully described.

The field is defined to be rectangular in shape with fixed dimensions and surrounded by a non-erodible border. Initially, the field is assumed to be homogeneous. That is, the soil characteristics are uniform, any plowed ridges are uniform, surface aggregates are uniform, any armoring of the surface is uniform, residues are uniformly distributed, the field is assumed to be uniformly flat and barriers have uniform height and porosity.

The model then overlays the field with a rectangular grid. The purpose of the grid is twofold. First, during an erosive event, surface changes do not occur uniformly throughout the field. Erosion tends to start near the windward edge of the field and progress across the field. Dividing the field into cells allows the assumption of a locally uniform surface to be maintained, ie. during the event the field becomes non-uniform but the cell is assumed to remain uniform. Second, the cells are used as an accounting device to track the displacement of soil. Both the soil that leaves the field and the soil that moves from one place in the field to another is accounted for.

Once the grid is in place, the actual simulation begins. ESM is driven by wind data. It assumes that the wind direction is constant for a 24 hour period with hourly wind speed inputs when called from WEPS. When called from SWEEP, the wind speed interval can be varied. The model also calculates its sweep pattern at this time. That is, the model determines the order of calculation for the grid cells. At each time step, the model starts with the most windward cell so that any soil displaced from one cell will be accounted for in an adjoining cell during the current time step.

The model takes the first interval wind speed and converts it to a friction velocity at the field location. Friction velocity is proportional to the momentum transfer of the wind to the surface and is calculated from the wind speed, surface aerodynamic roughness and vegetation silhouette. If the friction velocity is less than the minimum threshold friction velocity of the cells (threshold friction velocity is the minimum friction velocity for erosion to start) then the model immediately proceeds to the next hour's wind speed and notes that no erosion occurred during this hour.

If the friction velocity is greater than any cell's threshold friction velocity then erosion may occur. At this point a time step, usually less than the wind speed interval, is calculated. The model assumes quasi-steady stateness. That is, as the model proceeds through the cells, it calculates fluxes based upon the friction velocity and surface characteristics and integrates the mass change for the cell by multiplying the flux for the cell by the time step. There are three separate fluxes that are calculated and tabulated for different sized particles: saltation/creep, suspension and PM_{10}.

Once the accounting is done the cell surface characteristics are updated. This includes increasing or decreasing the reservoirs of saltation/creep, suspension and PM_{10} particles due to the effects of breakage from saltating aggregates, changing the aerodynamic roughness of the surface due to ridge degradation, etc. There is also a check to determine if there are limiting factors that may require the length of the next time step to be reduced.

Once time steps for the wind speed interval are completed, the next wind speed is used and the process continues. Once the 24 hours is over, the daily totals are calculated and stored and the routine returns. In WEPS, ESM is called sequentially after the other sub-models have completed on a daily time-step. In SWEEP, ESM is called just once. The daily simulation flow is illustrated in Fig. 1.

It is important to note that in WEPS the changes in the surface conditions from the movement of soil by wind are not yet used to update the soil surface for the following day. The homogenous soil surface conditions determined by the other submodels are used to reinitialize the grid cell values to start the next simulation day. This eliminates the need to divide the field into various subregions as the new nonuniform soil surface conditions will affect the simulation of crop growth, hydrology, decomposition, managment operations and climatic effects on soil conditions. Each daily erosion simulation is considered to be an independent trial of the soil and it's management, not of the cumulative effect of the erosion events. In addition, field studies have shown that 2-3 days after an erosion event,

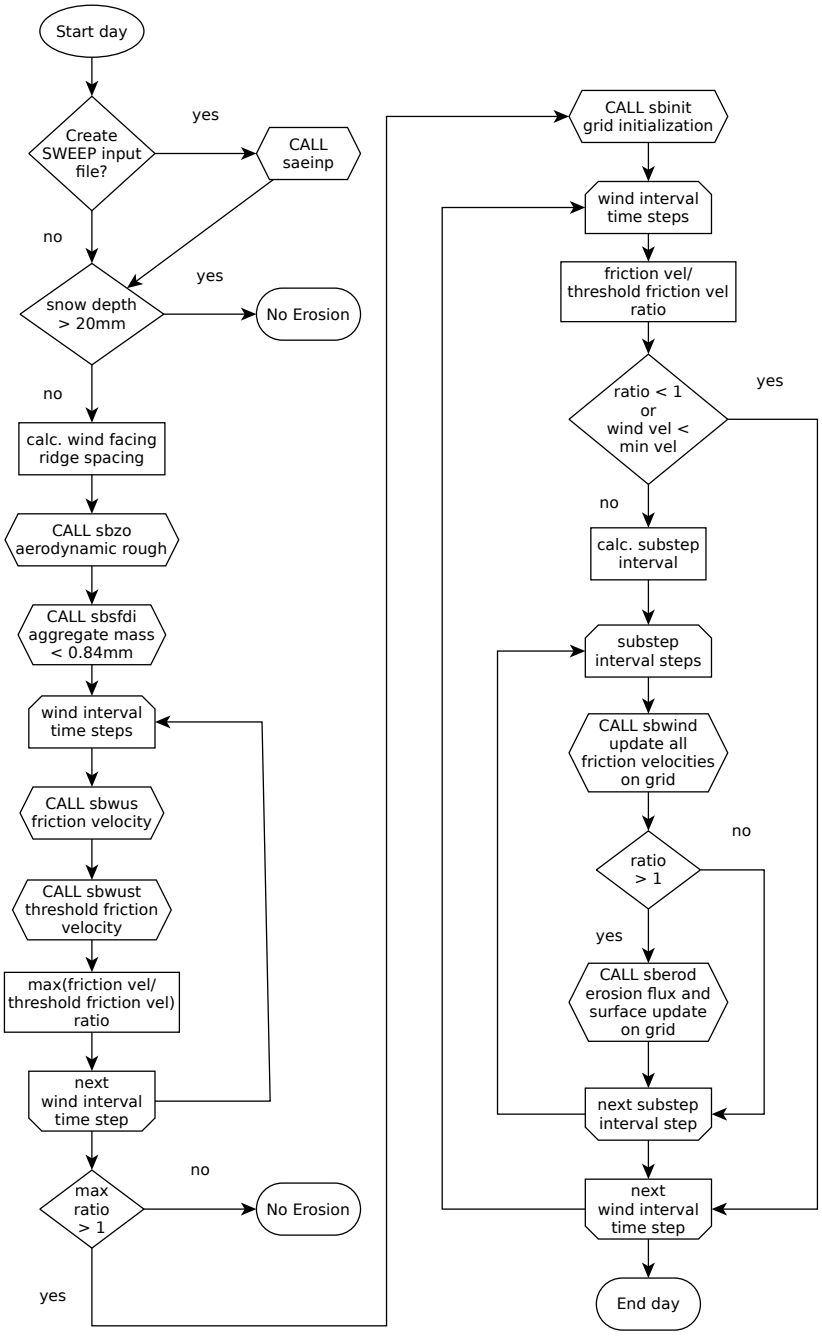

Fig. 1: Flowchart of erosion submodel execution logic.

the resevoirs of suspension sized particles have been observed to return to pre-event levels. Therefore, it seems more appropriate to re-initialize the surface parameters rather than keep the simulated results. Future research may justify retaining the change in surface conditions due to wind erosion events by creating subregions or averaging the changes.

3 Input Details

There are four basic types of inputs for ESM: field size and orientation, wind speeds and direction, wind barrier(s) and initial soil surface and layer characteristics.

3.1 Field (Physical Region)

In ESM, the erodible simulation region is rectangular in shape and surrounded by a boundary that does not allow moving soil in the saltation/creep transport mode to enter the simulation region from upwind, i.e. the erodible area is assumed to be surrouneded by a non-erodible boundary. (see Fig. 2). To facilitate calculations and accounting, a rectangular, not necessarily square, grid is generated that overlays the erodible simulation region. Erosion is calculated in individual grid cells using a single pass over all the cells. Using a single pass requires that the sequence of calculations be selected so that they always proceed along the downwind direction.

In WEPS 1.0 the generated grid has a maximum of size of interior 29 X 29 grid cells with a minimum of 7 m cell length. In narrow strips 3 grid cells are always generated, so the minimum cell length may be less than 7 m. The number of grid cells was restricted to reduce computation time but can easily be modified in the code. When barriers are present, the maximum is increased to 59X59. The increased number of grid cells is necessary to permit adequate resolution of the barrier reductions in the wind speed for sufficiently large fields. SWEEP allows for overiding the default number of grid cells using command line options.

3.2 Input Winds

Simulated, hourly, wind speeds ($\frac{m}{s}$) from a weather station representative of the simulation region are normally input to the sub-model. The wind speeds generated from the WEPS wind database are at a 10 m height (van Donk et al. 2005). The aerodynamic roughness at the weather stations is assumed to be 25 mm. For WEPS simulations using measured wind data, it needs to be adjusted to these conditions. A simulated daily wind direction is also input to the sub-model. ESM is not called unless maximum daily wind speed at 10 m height exceeds 8 $\frac{m}{s}$. By doing so, only major erosion events are simulated. Then the maximum daily wind speed is used to determine if erosion can occur in the simulation region. If snow depth exceeds 20 mm, no erosion is simulated. When the erosion submodel is called, a minimum wind speed is specificed, below which no erosion grid calculations are performed in an attempt to reduce erosion calculation overhead. When called from WEPS, the minimum wind speed is set to 5 $\frac{m}{s}$. When using the SWEEP interface to simulate a single erosion event, this value is defaulted to 5 $\frac{m}{s}$, but may be modified using a command line argument. Also in SWEEP, measured wind data at the simulation field or from other heights may be used as input to the sub-model by setting $wzoflg$ to 1, and entering the anemometer height. The aerodynamic roughness of the field will then be used to find the friction velocity.

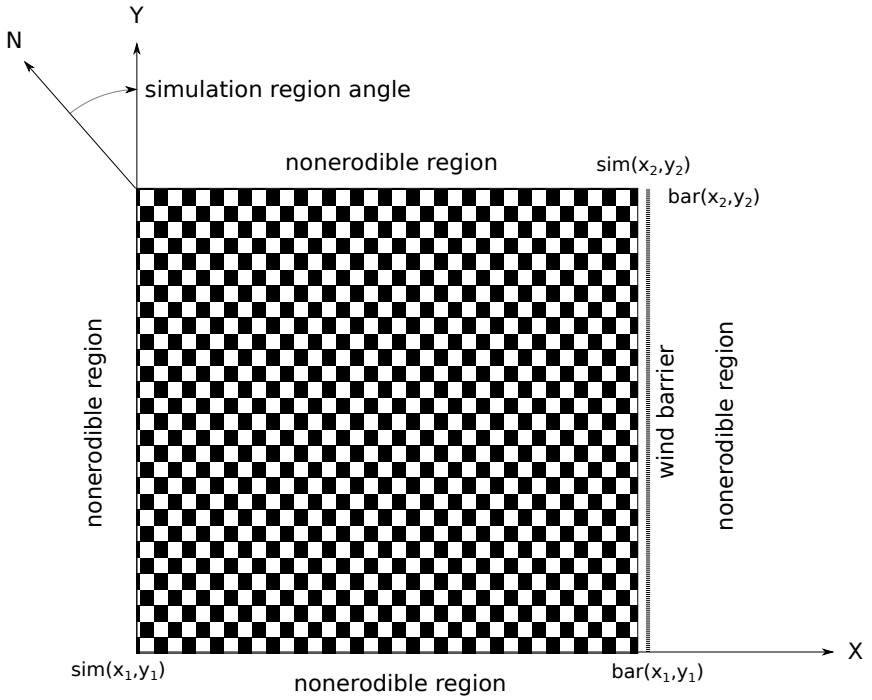

Fig. 2: Simulation region geometry in Cartesion coordinate system. The erodible region is a rectangle defined by the cartesian (x,y) coordinates of the opposite corners. Barriers are defined by the cartesian coordinates of the end points of the barrier. The simulation region and barriers are then referenced to true North by an angle of rotation. The simulation region is divided into grid cells for erosion calculations.

3.3 Wind Barriers

Up to five (limitation of present fortran code) wind barriers can be placed arbitrarily on erodible areas or boundaries of the simulation region (see Fig. 2). The sub-model inputs required to define each wind barrier include the locations of the barrier ends in simulation region coordinates, bar(x_1,y_1) and bar(x_2,y_2). Other inputs needed to define the barrier include the height, optical porosity, and total width of the barrier. (The user interface in WEPS 1.0 currently restricts the maximum number of barriers to four and allows them to be placed only on the simulation region boundaries. This restriction is expected to be removed in later interface versions that will allow the user to draw the barriers onto a geographic representation of the field. Barriers in the SWEEP interface are not restricted to the simulation region boundaries.)

3.4 Input Surface Conditions

The surface conditions considered are combinations of the following:

1. Surface roughness - random and/or oriented measured below the standing biomass canopy but on top of flat residues (Fig. 3);

2. Surface covers - flat, random, biomass cover; crust with loose, erodible soil on crust; aggregated soil; and rock cover (>2.0 mm dia.) (Fig. 4);

3. Surface soil moisture, crust/consolidated zone parameters (dry stability and thickness), aggregate parameters (dry stability and size distribution); and

4. Standing biomass parameters (leaf area index, stalk silhouette area index, height, row spacing, position on ridge, and orientation) (Fig. 5).

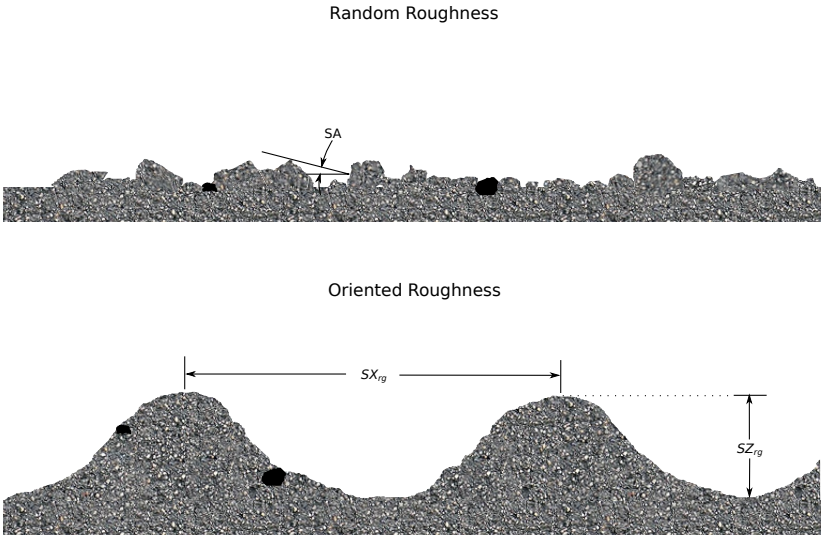

Fig. 3: Random roughness shelter angles (SA) and oriented roughness spacing (SX_{rg}) and height (SZ_{rg}) used in ESM.

The random roughness parameter is the standard deviation (mm) of the surface roughness below the biomass canopy and includes the roughness contributed by flat biomass.

The oriented roughness parameters include the ridge height, ridge spacing, top width of beds, furrow dike spacing and furrow dike height (mm). The latter are assumed to be the same height as the ridges. Based on the oriented and random roughness parameters, the horizontal fraction of surface area sheltered from saltation impacts is also calculated in the sub-model (Potter, Zobeck, and Hagen 1990). The saltation impact angle was assumed to be 12 *degrees* above horizontal.

Soil scientists in the U.S. generally report the sum of the soil mass fractions less than 2 mm diameter as 1.0 and then report volume of rocks as a separate value in their databases. As inputs to ESM, we have followed this precedent and let the numerical values of the surface fractions of crusted and aggregated soil sum to 1.0.

However, in applying surface cover in ESM, we assigned rock >2.0 mm, aggregated soil, and crusted soil as the first level of cover, and forced their effective fractions to sum to 1.0 (Fig. 4). The second level of cover was assigned as fraction of the crust covered with loose soil; the maximum for this fraction is 1.0. The third level was assigned as the biomass flat fraction of cover, which is assumed to have random distribution over the entire surface and has a maximum value of 1.0.

In addition to the cover fractions illustrated in Fig. 4, additional input parameters are used to describe the surface soil components. These include loose mass on the crust $\left(\frac{kg}{m^2}\right)$, crust dry stability $\left(\ln\left(\frac{J}{kg}\right)\right)$, and crust/consolidated zone thickness (mm). Aggregates are

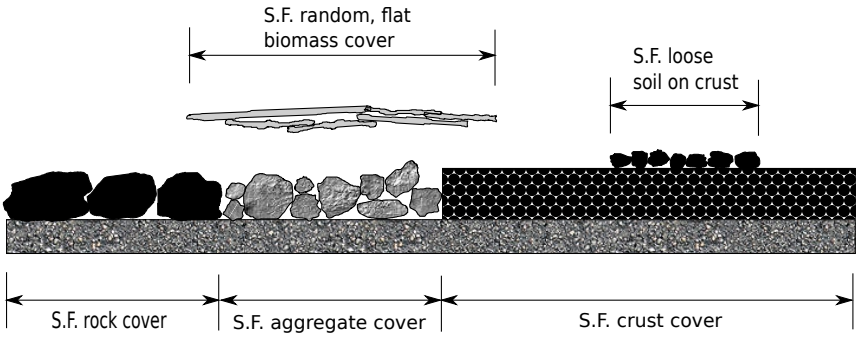

Fig. 4: Surface cover fraction (S.F.) descriptions used in ESM.

described by their dry aggregate stability $\left(\ln\left(\frac{J}{kg}\right)\right)$ (Hagen, Skidmore, and Saleh 1992) and their size distribution using a four parameter modified log-normal distribution function (Wagner and Ding 1994).

4 Physical Process Erosion Theory

The atmospheric boundary layer conditions most often encountered with the movement of soil by wind are best described as turbulent with neutral buoyancy. The wind velocity profile can then be described by the equation (Priestley 1959)

$$\frac{U}{U_*} = \frac{1}{K}\ln\left(\frac{Z - Z_d}{Z0}\right) \tag{1}$$

where

$U=$ wind velocity at height Z $\left(\frac{m}{s}\right)$

$U_*=$ friction velocity $\left(\frac{m}{s}\right)$

$K=$ Von Karmen's constant (approximately equal to 0.4)

$Z=$ height above the surface (mm)

$Z_d=$ zero-plane displacement (mm)

$Z0=$ aerodynamic roughness length (mm)

The friction velocity at the soil surface, defined as the square root of surface shear stress divided by the fluid density, is the primary expression of the force of the wind available to cause soil movement.

4.1 Processed Based Modeling

Process-based models use formulas derived from observations to calculate the amounts for a given set of input values and a given amount of time. In this model, erosion rates are the critical, observed values. The rate of erosion is assumed to be quasi-steady state.[1] It is also

[1] That is, for time periods of interest, the rate of erosion is constant.

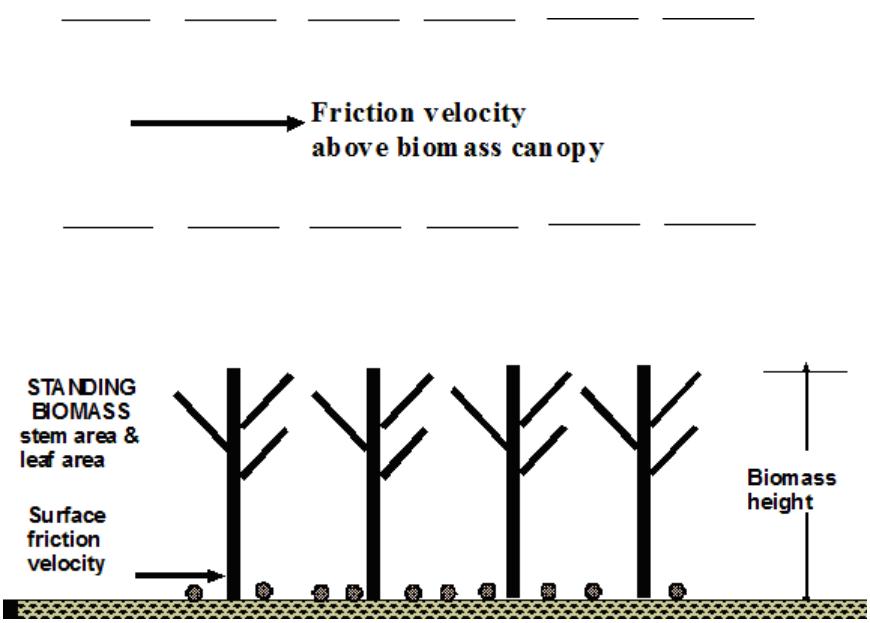

Fig. 5: Friction velocity above biomass canopy

assumed that there is a resevoir of erodible particles to which the erosion rate is applied. Obviously, this resevoir can be depleted during an erosive event. Not quite so obviously, there are processes during an erosion event that can replenish these resevoirs.

Soil transport during wind erosion occurs in three modes (Chepil and Woodruff 1963): creep-size aggregates (0.84 - 2.0 mm diameter) roll along the surface, saltation-size aggregates (0.10 - 0.84 *mm* diameter) hop over the surface, and suspension-size aggregates (<0.10 *mm* diameter) move above the surface in the turbulent flow. Obviously, as wind speeds, turbulence, or sediment loads change, the diameter of aggregates moving in the various modes also may change slightly (Pye 1987).

In ESM, we have assumed that the combined saltation/creep mode of transport has a distinct transport capacity for each surface, based on the surface roughness and wind speed. This assumption generally is supported by both field and wind tunnel measurements of the saltation/creep discharge (Greeley and Iverson 1985). We also assumed that the suspension component does not reach a transport capacity on most eroding fields. Given they respond differently to both the wind forces and sediment load (Gillette et al. 1997), separate equations were developed for saltation/creep, suspension, and PM_{10} (<0.01 *mm* diameter)[2] discharge. Separating these erosion components also is useful, due to their different potential off-site impacts.

Wind erosion occurs over a wide range of surface conditions. To aid in delineating erosion rates among the various surfaces, several individual erosion processes are identified in ESM (Hagen et al. 1995) (Fig. 6). These processes include direct entrainment (emission) of loose soil by wind and/or saltation impacts, abrasion of soil from clods/crust by saltation impacts, and breakage of saltation/creep-size aggregates to suspension-size. These processes differ from one another by approximately an order of magnitude in their ability to supply new suspension or saltation/creep-size mass to the airstream in response to a saltation

[2] PM_{10} is a subset of suspension that is of particular interest to EPA, et. al., due to the health consequences of breathing high concentrations of PM_{10}.

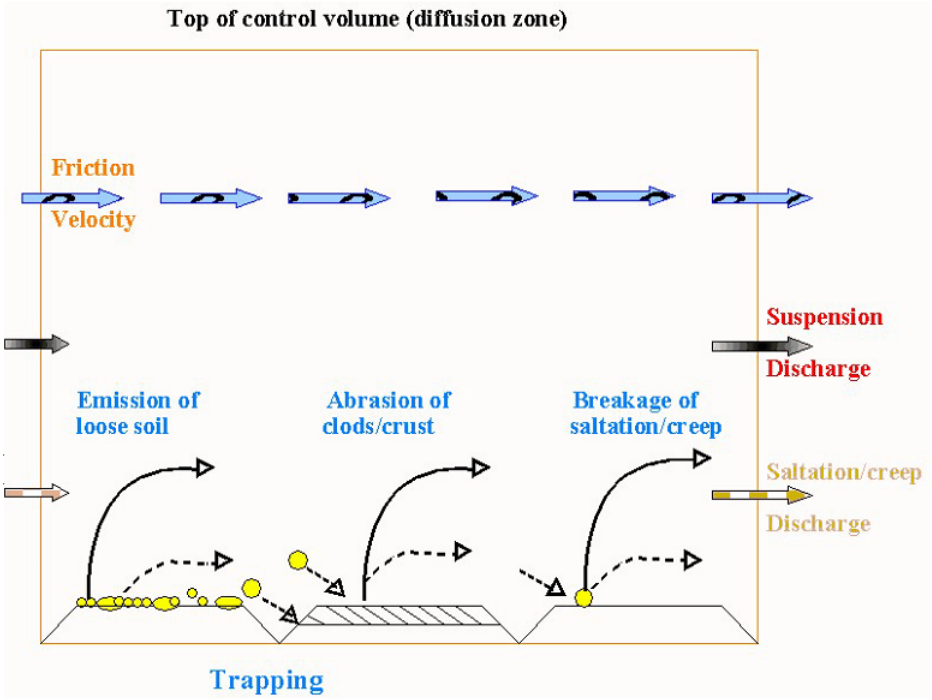

Fig. 6: Simulated erosion processes on a bare soil in an individual grid cell.

impact (Mirzamostafa et al. 1998) and are simulated individually. When the saltation/creep discharge exceeds transport capacity over cells in a local area of the surface, trapping of saltation/creep occurs. It is also assumed that the coarse fraction of the suspension component begins deposition when moving over cells in the simulation region that have standing residue or no active saltation and sufficient roughness.

Field surfaces vary both temporally and spatially. By partitioning complex areas into a series of small, uniform areas by gridding, and periodically updating the surface conditions, one may encompass both the spatial and temporal variations in fields. However, to simplify user inputs, the initial condition of the simulation region is assumed to have uniform soil and management. To meet stringent run-time requirements, the quasi-steady state solutions to mass conservation equations outlined in this section are used to predict wind erosion.

Finally, ESM uses the same grid for both spatial variation in the field and for accounting for soil movement. This allows the model to identify the areas in the field that experience wind erosion as well as total soil loss for the field as a whole.

4.2 Flux Equation

The following equations are used to calculate the boundary discharge, for the three components of erosion: saltation/creep, suspension and PM_{10}. The three are calculated separately since their formation and transport are largely independent processes. Note that there are two, distinct types of erosion flows being discussed: vertical fluxes that are for individual points and boundary discharges which integrate the point fluxes into line discharges. Further note that these solutions are applied to grid cells, not to the field as a whole. This implies that grid cells located on the edge of the field, i.e. adjacent to the non-erodible boundary, have no incoming loading when the wind is blowing in from that boundary. This

is an important distinction for the saltation/creep component which has a finite transport capacity but does not effect suspension or PM_{10} particles, where the model assumes an infinite transport capacity.

4.3 Saltation/creep component

Based on conservation of mass in a control volume (Fig. 6), a one-dimensional, quasi-steady state equation for the physical processes involved in saltation/creep is:

$$\frac{dq_{sc}}{dX} = G_{en} + G_{an} - Gss_{bk} - G_{tp} \tag{2}$$

where

q_{sc} = horizontal saltation/creep discharge $\left(\frac{kg}{m.s}\right)$

X = downwind distance from nonerodible boundary $(m) G_{en}$= vertical flux from emission of loose aggregates $\left(\frac{kg}{m^2 s}\right)$

G_{an}= vertical flux from abrasion of surface clods and crust $\left(\frac{kg}{m^2 s}\right)$

Gss_{bk}= vertical flux of suspension aggregates from breakage of saltation/creep aggregates $\left(\frac{kg}{m^2 s}\right)$

G_{tp}= vertical flux from trapping of saltation/creep aggregates $\left(\frac{kg}{m^2 s}\right)$

Each of the vertical fluxes represents either source or sink terms in the control volume and can be estimated by the equations that follow. The net emission source term for loose aggregates is:

$$G_{en} = (1 - SFss_{en})\, C_{en}\, (q_{en} - q_{sc}) \tag{3}$$

where

$SFss_{en}$= mass fraction of suspension-size ($< 0.10\, mm$) among loose aggregates ($< 2.0\, mm$ diameter)

C_{en}= coefficient of emission $\left(\frac{1}{m}\right)$

q_{en}= transport capacity $\left(\frac{kg}{m.s}\right)$

Stout (1990) derived the general form of Eq. 3 and applied it to describe total mass flux at a given height from the surface. However, subsequent research (Hagen 1991c) showed that the abrasion flux from immobile clods and crust was controlled by other factors. Hence, as described here, Eq. 3 applies only to the loose, mobile components of the soil. A typical value for C_{en} on a loose, bare field is about $0.06\left(\frac{1}{m}\right)$, and values for other conditions have been reported (Hagen et al. 1995). Many transport capacity equations for saltation/creep have been reported (Greeley and Iverson 1985). One of the most frequently used was developed by Lettau and Lettau (1978) which is expressed as

$$q_{en} = C_s\, (U_*)^2\, (U_* - U_{*t}) \tag{4}$$

where

C_s= the saltation transport parameter $\left(\frac{kg_{\bullet}s^2}{m^4}\right)$, with a typical value of about 0.3 or a greater value for surfaces armored with stones

U_*= friction velocity $\left(\frac{m}{s}\right)$

U_{*t}= dynamic threshold friction velocity $\left(\frac{m}{s}\right)$

The suspension-size aggregates are assumed to be mixed intimately with the saltation/creep-size and emitted with them. Although the suspension-size aggregates absorb part of the aerodynamic and impact energy (represented by the emission coefficient) in order to rise from the surface, they do not contribute toward reaching the transport capacity of saltation/creep. Hence, they are subtracted from the total emission of loose aggregates in Eq. 3. The net source term for entrainment of saltation/creep aggregates abraded from immobile aggregates and crust by impacting saltation/creep is

$$G_{an} = (1 - SFss_{an}) \left[\sum_{i=1}^{2} (F_{an_i} C_{an_i})\, q_{sc}\right] \left(\frac{q_{en} - q_{sc}}{q_{en}}\right) \tag{5}$$

where

$SFss_{an}$= mass fraction of suspension-size from abrasion

F_{an_i}= mass fraction saltation impacting clods and crust

C_{an_i}= coefficient of abrasion for pool i $\left(\frac{1}{m}\right)$.

i = pool index (1 - ag for aggregates, 2 - cr for crust)

An index of two was used in Eq. 5 since, in general, only two targets, exposed clods and crust, must be considered. Other targets, such as residue and rocks, have a C_{an_i} near zero. The first term, $(1 - SFss_{an})$, is the fraction of abraded mass that is of saltation/creep-size. Values of $SFss_{an}$ for some Kansas soils have been measured and ranged from 0.14 to 0.27, depending upon soil texture (Mirzamostafa 1996). The middle, bracketed term on the right-hand-side of Eq. 5 represents the total soil abraded from clods and crust, as confirmed by wind tunnel experiments (Hagen 1991c). Values for C_{an_i} also have been measured for a range of soils and related to their crushing energy (Hagen, Skidmore, and Saleh 1992). The final term in Eq. 5 is the mass fraction entrained in the air stream. Note that the entrainment rate of this newly created saltation/creep is assumed to be similar to that of loose, saltation/creep-size aggregates already present on the surface, and that the entrainment approaches zero at transport capacity.

A sink for the saltation/creep discharge occurs when these aggregates are broken into suspension-size (Mirzamostafa et al. 1998). This effect is simulated as

$$Gss_{bk} = C_{bk}\,(q_{sc} - q_s) \tag{6}$$

where

C_{bk}= coefficient of breakage $\left(\frac{1}{m}\right)$

q_s= discharge of primary (non-breakable) sand particles $\left(\frac{kg}{m_{\bullet}s}\right)$

The discharge of primary sand particles, q_s, is approximated using

$$q_s = SF_{san} q_{sc} \tag{7}$$

where

SF_{san}= surface soil fraction sand

resulting in a soil sand fraction term in the calculation of the breakage coefficient. The saltation/creep aggregates are more stable than the surface clods and crust, so measured abrasion coefficients average about 9 times more than the breakage coefficients on the same soils (Mirzamostafa 1996). The wind tunnel experiments also demonstrated that the breakage coefficient remained constant during breakdown of the aggregates to primary particles. The means and variances of these coefficients are related to soil texture. Given q_{sc}, values for q_s can be estimated directly from soil sand content as in Eq. 7.

Another sink term is the removal of saltation/creep from the air stream by trapping mechanisms (Hagen and Armbrust 1992). In WEPS, surface trapping and plant interception are simulated as

$$G_{tp} = C_t \left(1 - \frac{q_{cp}}{q_{en}}\right) q_{sc} + C_i q_{sc},\ q_{en} \geq q_{cp} \tag{8}$$

where

C_t= coefficient of surface trapping $\left(\frac{1}{m}\right)$

C_i= coefficient of plant interception $\left(\frac{1}{m}\right)$

q_{cp}= transport capacity of the surface $\left(\frac{kg}{m \cdot s}\right)$

When erosive winds cross rough surfaces, such as tillage ridges, that are highly erodible, large amounts of soil are entrained, but a portion of the entrained saltation/creep is often trapped in succeeding downwind furrows. This phenomenon results in a local rearrangement of the surface and reduces net removal of the entrained soil. Our conventionally-defined transport capacity, q_{en}, is based on the threshold velocity where erosion begins. But, when trapping of saltation/creep occurs on rough surfaces, one may hypothesize that q_{en} has been exceeded, and that the true transport capacity of the surface is some value, q_{cp}, that is less than q_{en}. However, q_{en} still appears to be the appropriate limiting value to drive the emission process, because more soil is emitted than can be transported from the local area. In WEPS, the first term on the right-hand-side of Eq. 8 simulates trapping of saltation/creep by surface roughness. The true transport capacity of the surface, q_{cp}, is based on the threshold friction velocity needed to remove saltation/creep from the furrows. It is calculated using Eq. 4 for a given roughness at the level of clod and crust cover of the surface.

$$q_{cp} = C_s \left(U_*\right)^2 \left(U_* - U_{*tt}\right) \tag{9}$$

where

U_{*tt}= dynamic threshold friction velocity of bare surface$\left(\frac{m}{s}\right)$

The second term of Eq. 8 represents interception of saltation/creep by standing plant stalks or other near-surface plant parts. For a given soil surface friction velocity, more transport occurs without than with stalks. Also, the transport capacity is higher when the wind

direction is parallel to crop rows than when the wind direction is perpendicular to rows. For saltation normal to the row direction, interception can reduce transport capacity from 5 to 10 percent (see Eq. 113). Comparisons to measured data have been reported previously (Hagen and Armbrust 1994).

4.4 Solution for saltation/creep discharge

When the source and sink terms are collected on the variable q, Eq. 2 for saltation/creep can be written in the form

$$\frac{dq_{sc}}{dX} = A + Bq_{sc} - C\left(q_{sc}\right)^2 \tag{10}$$

where

$$A = \left(1 - SFss_{en}\right) C_{en} q_{en} \tag{11}$$

$$\begin{aligned} B = \left(1 - SFss_{an}\right) \left[\sum_{i=1}^{2} (F_{an_i} C_{an_i})\right] - \left(1 - SFss_{en}\right) C_{en} \\ -C_{bk} - C_t \left(1 - \frac{q_{cp}}{q_{en}}\right) - C_i \end{aligned} \tag{12}$$

$$C = \left(1 - SFss_{an}\right) \left[\sum_{i=1}^{2} \left(F_{ani} C_{ani}\right)\right] \left(\frac{1}{q_{en}}\right) \tag{13}$$

Integrating Eq. 10 along the wind direction, from X_1 to X_2 and q_{sc1} to q_{sc2}, gives the solution

$$q_{sc2} = \frac{S}{2C} \left(-\tanh\left(t_1\right) + \frac{B}{S}\right) \tag{14}$$

where

$$t_1 = \begin{cases} \frac{S}{2}\left(-\triangle X\right) + 0.5 \ln\left(\frac{1+p}{1-p}\right), & -1 < p < 1 \\ -20, & p \le -1 \\ 20, & p \ge 1 \end{cases} \tag{15}$$

$$S = \sqrt{4AC + B^2} \tag{16}$$

$$p = \frac{-2Cq_{sc1} + B}{S} \tag{17}$$

$$\triangle X = \left(X_2 - X_1\right) \tag{18}$$

The distance that the wind travels across a grid cell, $\triangle X$ is calculated from the uniform grid cell spacing and wind direction. It is adjusted to an effective distance to account for the effects of moving diagnoally across a rectangular cell as

$$\triangle X = ld \times \left(1 - 0.292893 \frac{la \times lb}{ix \times jy}\right) \tag{19}$$

$$\left\{\begin{array}{c} la = jy \\ lb = |\tan(awa) \times jy| \\ ld = \left|\frac{jy}{\cos(awa)}\right| \end{array}\right\}, \quad |\tan(awa)| \leq \frac{ix}{jy}$$
$$\left\{\begin{array}{c} la = \sqrt{ld^2 - lb^2} \\ lb = ix \\ ld = \left|\frac{ix}{\sin(awa)}\right| \end{array}\right\}, \quad |\tan(awa)| > \frac{ix}{jy} \tag{20}$$

$$awa = WA_{dir} - amasim \tag{21}$$

where

$\triangle X$ = effective distance wind travels across grid cell (m)

ix = grid cell spacing in the x direction (m)

jy = grid cell spacing in the y direction (m)

awa = wind direction relative to the simulation region y-axis ($degrees$)

$amasim$ = angle of the simulation region y-axis relative to geographic north ($degrees$)

WA_{dir} = wind direction relative to geographic north ($degrees$)

4.5 Suspension component

Based on conservation of mass in a control volume that extends to the top of the dust cloud, a one-dimensional, quasi-steady state equation for the physical processes generating the suspension component is

$$\frac{dq_{ss}}{dX} = (Gss_{en} + Gss_{an} + Gss_{bk})(1 - Css_i),\ U_* > U_{*t} \tag{22}$$

or

$$\frac{dq_{ss}}{dX} = -Gss_{dp},\ U_* < U_{*t} \tag{23}$$

where

q_{ss}= horizontal suspension component discharge $\left(\frac{kg}{m \cdot s}\right)$

Gss_{en} = vertical emission flux of loose, suspension-size aggregates $\left(\frac{kg}{m^2 s}\right)$

Gss_{an}= vertical flux of suspension-size aggregates created by abrasion of clods and crust $\left(\frac{kg}{m^2 s}\right)$

Gss_{bk}= vertical flux of suspension-size aggregates created by breakage of saltation/creep-size aggregates $\left(\frac{kg}{m^2 s}\right)$

Css_i= fraction of suspension-size aggregate flux intercepted by standing biomass

Gss_{dp}= vertical flux (deposition) of suspension-size aggregates above a non- eroding surface $\left(\frac{kg}{m^2 s}\right)$

The source and sink terms for the suspension component are simulated by the equations that follow. For direct emission of loose, suspension-size material by 'splash' impacts and aerodynamic forces

$$Gss_{en} = SFss_{en} C_{en} \left(q_{en} - q_{sc}\right) + C_m q_{sc} \tag{24}$$

where

C_m= a coefficient of mixing, value about$(0.0001\, SFss_{en})$ $\left(\frac{1}{m}\right)$

Below transport capacity, the driving force causing the emission flux of suspension-size soil is assumed to be similar to that in Eq. 3 causing the saltation/creep emission flux. This assumption is supported by wind tunnel measurements that show a mixture of suspension-size aggregates and a mixture of saltation-size have about the same threshold velocities (Chepil 1951). However, two additional assumptions are inherent in Eq. 24. The first is that the loose components of saltation/creep and suspension-size aggregates occur as a uniform mixture in the field. As a consequence, during simple net emission, the suspension fraction emitted with the saltation/creep remains the same as it was in the soil. Hence, the suspension fraction can be estimated as

$$SFss_{en} = \frac{SFss}{SFer} \tag{25}$$

where

$SFss$= soil mass fraction of loose, suspension-size less than about 0.1 mm

$SFer$= soil mass fraction of loose, erodible-size, less than about 2.0 mm

The second assumption in Eq. 24 is that an additional small amount of suspension-size aggregates that are disturbed by the saltation impacts also are entrained, because transport capacity for the suspension component generally is not limiting. The result of this process is gradual depletion of the loose, suspension-size aggregates at the surface. However, when net emission of suspension-size exceeds net emission of saltation/creep-size aggregates, the latter soon dominate the surface area and absorb the impacts, so the process tends to be self-limiting.

For suspension flux created by abrasion of clods and crust,

$$Gss_{an} = SFss_{an} \left[\sum_{i=1}^{2} \left(F_{an_i} C_{an_i}\right)\right] q_{sc} \tag{26}$$

Additional discussion and measurements of this source term were reported by Mirzamostafa et al. (1998). For the source of suspension flux created by breakage of saltation/creep aggregates, the term is the same as the sink term in the saltation/creep equation and simulated as

$$Gss_{bk} = C_{bk} \left(q_{sc} - q_s\right) \tag{27}$$

Breakage from impact on immovable targets is assumed to come only from the impacting saltation/creep alone. Breakage coefficients for saltation-size aggregates have been measured in the wind tunnel (Mirzamostafa et al. 1998). But the breakage component from impacts on other saltation/creep is assumed to come from both the impacting and target aggregates. Breakage from impact on a mobile target is less likely than breakage

from impact on immobile targets. However, these assumptions need further experimental verification.

Finally, the sink term for trapping of suspension flux occurs when the suspension discharge passes over grid cells without active saltation to maintain the suspension flux from the surface. Typically, this implies the presence of a vegetated, water, or rough armored surface. The largest suspension particles, 0.05 to 0.10 mm, comprise roughly half the mass of the suspension discharge (Chepil 1951; Zobeck and Fryrear 1986). Through diffusion and settling, they move rapidly toward noneroding surfaces in the simulation region, which serve as sinks. The process is simulated as

$$Gss_{dp} = -C_{dp} q_{ss},\ q_{ss} > 0.5 q_{ss0} \tag{28}$$

where

q_{ss0}= maximum value of q_{ss} entering deposition region $\left(\frac{kg}{m \cdot s}\right)$

C_{dp}= coefficient of deposition of suspension-size $\left(\frac{1}{m}\right)$

The maximum value of C_{dp} is about 0.005, but less for smooth surfaces or large upwind areas that produce high dust clouds thus, moving a large portion of the soil away from the deposition surface.

4.6 Solution for suspension discharge

When the source terms are collected, Eq.22 can be written in the form:

$$\frac{dq_{ss}}{dX} = F + G\, q_{sc} \tag{29}$$

$$F = \left(SFss_{en} C_{en}\right)\left(1 - Css_i\right) q_{en} \tag{30}$$

$$\begin{aligned} G = \Bigg(& -SFss_{en} C_{en} + SFss_{an} \left[\sum_{i=1}^{2} \left(F_{an_i} C_{an_i}\right)\right] \\ & + C_{bk} + C_m \Bigg)\left(1 - Css_i\right) \end{aligned} \tag{31}$$

Substituting the general solution of Eq. 2, $q(X)$, into Eq. 29 and integrating along the wind direction from X_1 to X_2 and q_{ss1} to q_{ss2} gives the following equation for suspension discharge

$$\begin{aligned} q_{ss2} = q_{ss1} + \frac{1}{2C} & \left(\left(-G \cdot S + G \cdot B + 2F \cdot C\right)\left(\triangle X\right)\right) \\ & + 2G\left(-\ln\left(2\right) + \ln\left(\exp\left(S\left(\triangle X\right)\right)\left(1 - P\right) + P + 1\right)\right) \end{aligned} \tag{32}$$

In regions of deposition of suspension component, integration of Eq. 29 from location X_1, with discharge q_{ss1}, gives the following for suspension discharge, q_{ss2}, at downwind location X_2

$$q_{ss2} = q_{ss1} \exp(-C_{dp}(\triangle X)) \tag{33}$$

A value of $C_{dp} = 0.005$ in equation 33 matches the deposition measured at about 100 meters downwind of the eroding field at Big Spring; it under predicts deposition closer to the boundary. However the stable downwind area had considerable standing vegetation that made it a more effective sink than a smoother downind surface (Hagen et al. 2007). For a typical size distribution of suspended dust, only about 50 percent will likely be deposited near an eroding source field, thus the limitation in equation 28. In the future, C_{dp} should be a function of downwind aerodynamic roughness and perhaps a more complicated deposition equation.

4.7 PM_{10} component

Simulation equations for particles with aerodynamic diameters less than 10 μm (PM_{10} component) of the suspended soil also were developed by Hagen, Mirzamostafa, and Hawkins (1996). Three different sources of PM_{10} were identified to contribute different fractions of PM_{10} from the suspension generated from each source. This results in the parameterized equation

$$\frac{dq10}{dX} = SF10_{en}Gss_{en} + SF10_{an}Gss_{an} + SF10_{bk}Gss_{bk} \tag{34}$$

where

$SF10_{en}$= soil fraction of PM_{10} in suspension-size surface soil

$SF10_{an}$= soil fraction of PM_{10} in suspension-size aggregates created during abrasion of clods and crust

$SF10_{bk}$= soil fraction of PM_{10} in suspension-size aggregates broken from saltation and creep-size aggregates.

4.8 Solution for PM_{10} discharge

When the source terms are collected, Eq. 34 can be written in the form:

$$\frac{dq10}{dX} = H + K\, q_{sc} \tag{35}$$

where

$$H = SF10_{en}F \tag{36}$$

and

$$\begin{aligned} K &= SF10_{en}(C_m - SFss_{en}C_{en}) \\ &+SF10_{an}SFss_{an}\left[\sum_{i=1}^{2}(F_{an_i}C_{an_i})\right] + SF10_{bk}C_{bk} \end{aligned} \tag{37}$$

Substituting the general solution of Eq. 2, $q(x)$, into Eq. 34 and integrating along the wind direction from X_1 to X_2 and $q10_1$ to $q10_2$ gives the following equation for PM_{10} discharge.

$$\begin{aligned} q10_2 &= q10_1 + \frac{1}{2C}\left((-K\,.\,S + K\,.\,B + 2H\,.\,C)\,(\triangle X)\right) \\ &+2K\left(-\ln(2) + \ln\left(\exp\left(S\,(\triangle X)\right)(1-P) + P + 1\right)\right) \end{aligned} \tag{38}$$

5 Cell Parameters

The analytic solutions presented in the prior sections for erosion fluxes in each cell require a number of parameters. These parameters were derived from a wide range of experimental data. Parameters are summarized in the following sections for:

a) aerodynamic roughness, b) friction velocity, c) wind barriers, d) threshold friction velocity, e) emission parameters, f) abrasion parameters, g) breakage parameters, and h) trapping and interception parameters.

5.1 Aerodynamic Roughness

In WEPS, friction velocity drives erosion, but the meteorological input parameter is wind speed. For any given wind speed under neutral atmospheric conditions in the surface boundary layer, friction velocity is proportional to the natural logarithm of the surface aerodynamic roughness (Panofsky and Dutton 1984). To determine friction velocity, the aerodynamic roughness term of the log-law wind speed profile must be determined. For surfaces without standing biomass, the surface aerodynamic roughness is controlled by roughness of both the soil and flat biomass cover. In ESM, tillage ridges are characterized by their height, spacing, orientation, top bed width and the spacing of furrow dikes. The dike height is not used in this calculation, but is always by definition less than the ridge height. For ridge heights greater than 5 mm, The normalized aerodynamic roughness for ridges was found by Hagen and Armbrust (1992) to be (Fig. 7):

$$\frac{Z0_{rg}}{SZ_{rg}} = \begin{cases} \dfrac{1}{-64.1 + 135.5hl + \frac{20.84}{\sqrt{hl}}}, & SZ_{rg} > 5 \\ 0 & SZ_{rg} \leq 5 \end{cases} \tag{39}$$

where

$Z0_{rg}$= aerodynamic roughness of the ridges (mm)

hl = ridge height divided by ridge spacing

The ratio of ridge height to ridge spacing is limited to a maximum of 0.2, an estimate of the limitations of soil and the formation of ridges by tillage.

$$hl = \min\left(0.2, \frac{SZ_{rg}}{SXP_{rg}}\right) \tag{40}$$

where

SZ_{rg}= ridge height (mm)

SXP_{rg}= ridge spacing parallel the wind direction (mm)

When the wind direction is not perpendicular to the ridges, the effective ridge spacing is increased. When furrow dikes are present, and the wind is more parallel to the furrows, the effective ridge spacing is limited to the dike spacing. Additionally, with the effect of turbulence, the aerodynamic roughness of ridges never completely disappears when the wind is completely parallel to the ridges. This is approximated by limiting the sine of the angle to $\geq$0.1. The effective ridge spacing parallel to the wind direction is found by:

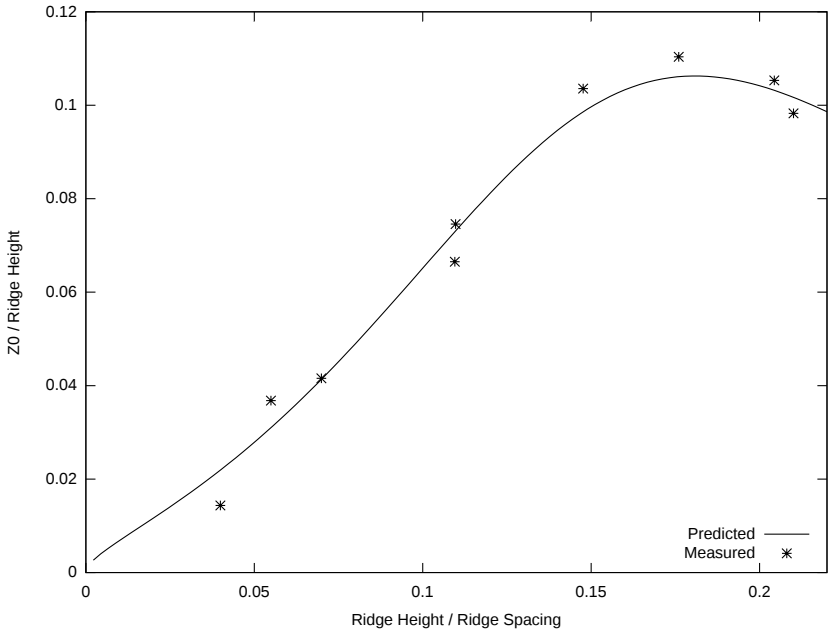

Fig. 7: Ratio of aerodynamic roughness to ridge height as a function of the ridge height to spacing ratio; Predicted is Eq. 39; Measured is from Hagen and Armbrust (1992).

$$SXP_{rg} = \begin{cases} \min\left(SX_{dk},\ \dfrac{SX_{rg}}{\max(0.1, |\sin(|WA_{dir} - SA_{rg}|)|)}\right), & SX_{dk} > \frac{SX_{rg}}{3} \\ \dfrac{SX_{rg}}{\max\left(0.1, |\sin(|WA_{dir} - SA_{rg}|)|\right)}, & SX_{dk} \leq \frac{SX_{rg}}{3} \end{cases} \tag{41}$$

where

SX_{rg}= ridge spacing (mm)

SX_{dk} = furrow dike spacing (mm)

WA_{dir}= wind direction relative to geographic north $(degrees)$

SA_{rg}= ridge orientation, clockwise from north and parallel to the ridge$(degrees)$

The resulting relationship for aerodynamic roughness as a function of all these limits is shown in Fig. 8.

Random roughness without standing biomass is limited to the range 1.67 to 100 mm, ie. 0.5 to 30mm equivalent aerodynamic roughness. Aerodynamic roughness is found from random roughness using

$$Z0_{rr} = \min\left(30,\ \max\left(0.5,\ 0.3\, SZ_{rr}\right)\right) \tag{42}$$

where

$Z0_{rr}$= aerodynamic roughness of random roughness including any flat biomass cover (mm)

SZ_{rr}= random roughness (mm)

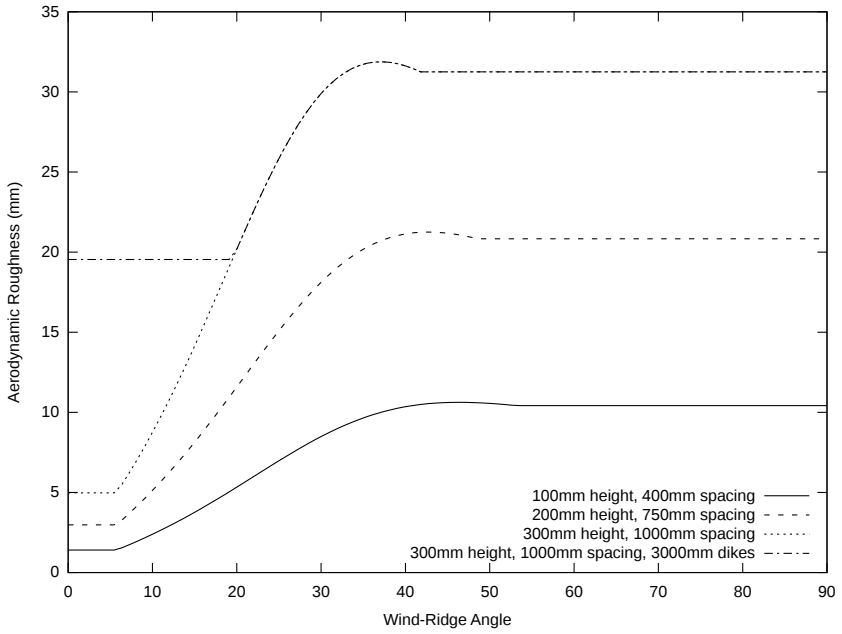

Fig. 8: Aerodynamic roughness as a function of the angle between the wind direction and ridge direction for several sample ridge heights, ridge spacings and dike spacings.

The aerodynamic roughness for the soil surface, $Z0$, calculated as the maximum of the ridge and random aerodynamic roughness is expressed as

$$Z0 = \max\left(Z0_{rg}, Z0_{rr}\right) \tag{43}$$

If standing plant biomass is present, the aerodynamic roughness length of the canopy is calculated from a biomass drag coefficient. Some crops are planted in a ridged field in the bottom of the furrow, resulting in a reduction of biomass drag. The biomass drag is also reduced when rows are spaced more than 5 times the biomass height. The standing biomass is considered composed of two parts, the current growing crop, and all other decomposing biomass. First, effective leaf and stem area indexes are calculated for all standing biomass as

$$BR_{lai} = R_{crow} R_{rg} C_{lai} + BD_{lai} \tag{44}$$

and

$$BR_{sai} = R_{rg} C_{sai} + BD_{sai} \tag{45}$$

where

BR_{lai}= biomass effective leaf area index $\left(\frac{m^2}{m^2}\right)$

BR_{sai}= biomass effective stem area index $\left(\frac{m^2}{m^2}\right)$

BD_{lai}= decomposing biomass leaf area index $\left(\frac{m^2}{m^2}\right)$

BD_{sai}= decomposing biomass stem area index $\left(\frac{m^2}{m^2}\right)$

C_{lai}= growing crop leaf area index $\left(\frac{m^2}{m^2}\right)$

C_{sai}= growing crop stem area index $\left(\frac{m^2}{m^2}\right)$

R_{crow}= reduction of effective leaf area due to crop row spacing (generally no effect until spacing is ¿ 5 crop heights)

R_{rg}= reduction of effective leaf and stem area when crop partly sheltered in furrow

Empirical estimates of the reduction factors are

$$R_{crow} = \begin{cases} \min\left[1, \frac{1}{0.92 + \frac{0.021 CX_{row}}{CZ - 0.5 SZ_{rg}}}\right], & CZ > .5SZ_{rg} \\ 0, & CZ \leq .5SZ_{rg} \end{cases} \tag{46}$$

and

$$R_{rg} = \begin{cases} 1.0 - \frac{.5SZ_{rg}}{CZ}, & CZ > .5SZ_{rg} \\ 0, & CZ \leq .5SZ_{rg} \end{cases} \tag{47}$$

where

CZ= growing crop height (m)

CX_{row}= growing crop row spacing (m)

SZ_{rg}= ridge height (m)

Leaves tend to orient parallel to the wind streamlines (Armbrust and Bilbro 1997) and the effective biomass drag coefficient as a function of leaf and stem area indexes is adjusted to reflect this as

$$BR_{cd} = 0.2 BR_{lai}(1.0 - \exp(-BR_{lai})) + BR_{sai} \tag{48}$$

where

BR_{cd}= effective biomass drag coefficient

The standing biomass aerodynamic roughness as a function of the effective biomass drag coefficient is taken from Hagen and Armbrust (1994)and calculated for an average stem diameter of 20 mm. While aerodynamic roughness may decrease slightly with decreased stem diameter, the effect of varying stem diameter is considered small enough to be neglected. For low values of the effective biomass drag coefficient, the roughness of the underlying surface will influence the canopy aerodynamic roughness as well, with the aerodynamic roughness with a canopy present never being less than the aerodynamic roughness of the underlying soil surface. For $BR_{cd} > 0.1$, the aerodynamic roughness of standing biomass is found using

$$Z0_v = \frac{BZ}{17.27 - \frac{1.254 \ln(BR_{cd})}{BR_{cd}} - \frac{3.714}{BR_{cd}}} \tag{49}$$

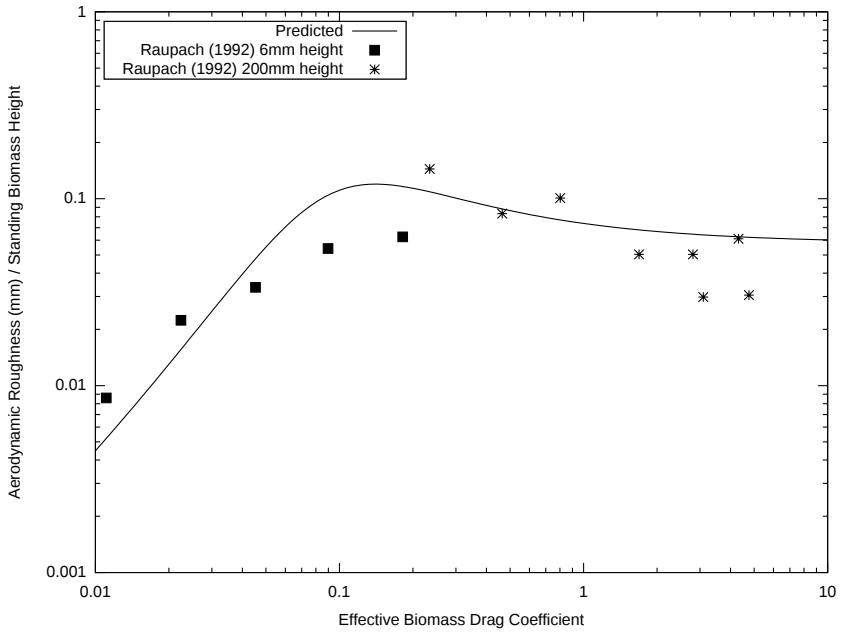

Fig. 9: The aerodynamic roughness / vegetation height ratio from equation 49 and the data from Raupach (1992), drag elements with both 6 mm and 200 mm heights mounted on a smooth substrate.

This relationship and the data from which it was derived are shown in figure 9. When $BR_{cd} \leq 0.1$, the relationship is affected by the vegetation height becoming

$$Z0_v = \begin{cases} BZ\left(\dfrac{Z0}{BZ} + \dfrac{0.11 - \frac{Z0}{BZ}}{4.60517}\ln\left(\dfrac{BR_{cd}}{0.001}\right)\right) & BZ > 5\, and\, BR_{cd} > 0.001 \\ 0 & BZ \leq 5\, or\, BR_{cd} \leq 0.001 \end{cases} \tag{50}$$

Finally, the aerodynamic roughness cannot be less than the roughness of the underlying surface becoming

$$Z0_v = \max\left(Z0_v, Z0\right) \tag{51}$$

The interactive effect of stem height and the underlying aerodynamic roughness on the aerodynamic roughness is illustrated in figure 10.

5.2 Friction Velocity

Friction velocity at the simulation region is calculated in two steps. First, the friction velocity at the weather station, where wind speeds are measured, is calculated for strong winds with neutral stability using the log-law profile (Panofsky and Dutton (1984)):

$$U_{*st} = \frac{0.4U_{st}}{\ln(\frac{Z_{st}}{Z0_{st}})} \tag{52}$$

where

U_{*st}= friction velocity at the weather station $(\frac{m}{s})$

U_{st}= wind speed at weather station $(\frac{m}{s})$

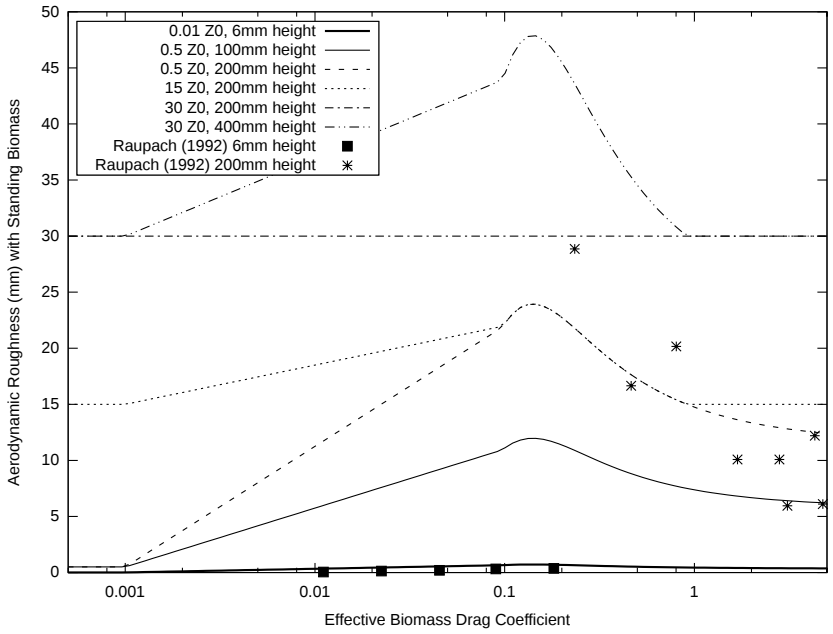

Fig. 10: Aerodynamic roughness with standing biomass as a function of effective biomass drag coefficient with various levels of Z0, the aerodynamic roughness of the underlying surface; Predicted is Eq. 49, 50, and 51; Data from Raupach (1992) are rods used to simulate standing stems.

Z_{st}= anemometer height at the weather station (mm); (wind speeds were adjusted to 10 m height in WEPS data base)

$Z0_{st}$= aerodynamic roughness at weather station, assumed to be 25 mm in WEPS

Second, the friction velocity at the simulation region is calculated based on the ratio of aerodynamic roughness at the simulation region to that at the wind speed measurement station. This equation is an approximation of a procedure suggested by Letteau (Panofsky and Dutton 1984).

$$U_{*v} = U_{*st}\left(\frac{Z0_v}{Z0}\right)^{0.067} \tag{53}$$

where

U_{*v}= friction velocity above the surface including any standing biomass $\left(\frac{m}{s}\right)$

$Z0_v$= as defined by equations 49, 50, and 51

If there is sufficient standing biomass, the friction velocity at the soil surface is calculated (Fig. 11) (Hagen and Armbrust 1994) as

$$U_* = \min\left(1, U_{*v}\left(0.86\exp\left(\frac{-BR_{cd}}{0.0298}\right) + 0.25\exp\left(\frac{-BR_{cd}}{0.356}\right)\right)\right) \tag{54}$$

where

U_*= friction velocity at soil surface below standing biomass $\left(\frac{m}{s}\right)$

At this point in the calculations, the influence of barriers or hills on friction velocity are still neglected.

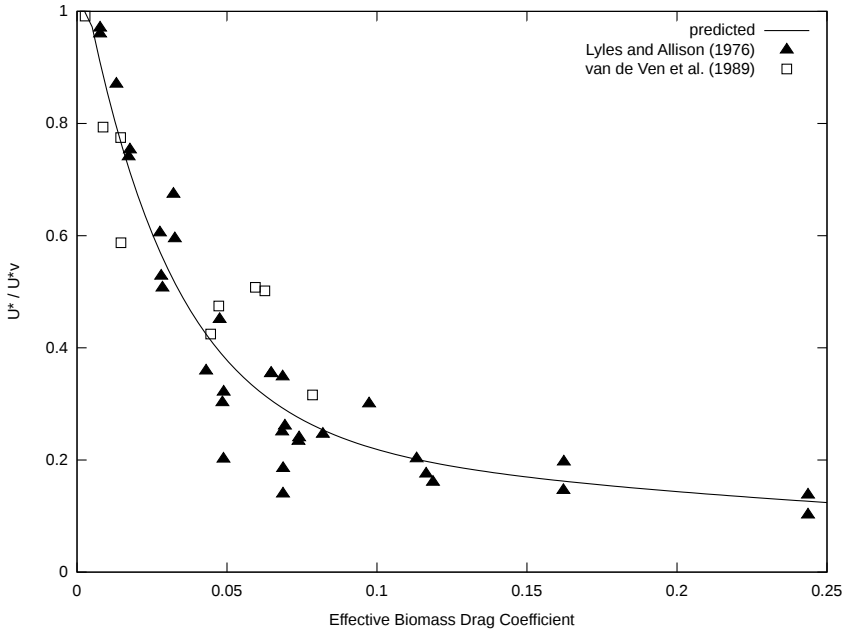

Fig. 11: Reduction in friction velocity through biomass canopy as a function of biomass drag coefficient; Predicted is Eq. 54; Data are Lyles and Allision (1976) and van de Ven, Fryrear, and Spaan (1989).

5.3 Wind Barrier Parameters

Wind barriers, e.g. trees, hedgerows, trap strips, snow fences, etc., create upwind and downwind sheltered areas. ESM treats barriers as overlays on the grid as opposed to creating non-erodible cells in the grid. The barrier effects are simulated by calculating the fraction of open field friction velocity that occurs in the portion of the simulation region that is sheltered by barriers. When two barriers shelter the same area, the lowest fraction of open field friction velocity created by a single barrier is selected for the grid cell for each wind direction. An analysis of field windbreak systems using this procedure was reported by Vigiak et al. (2003).

The rectangular simulation region has a y-axis positioned within ±45 degrees from north. Wind directions relative to the y-axis are calculated for 8 cardinal wind directions as:

$$awar_k = 45(k-1) - amasim \tag{55}$$

where

k = index of cardinal wind directions in clockwise direction (k=1 is north)

$awar_k$ = cardinal wind direction k relative to the simulation region y-axis ($degrees$)

$amasim$ = angle of the simulation region y-axis relative to geographic north ($degrees$)

Only 8 cardinal directions were selected for computational efficiency, being a precalculation done only once per simulation. Wind direction from WINDGEN is provided for the 16

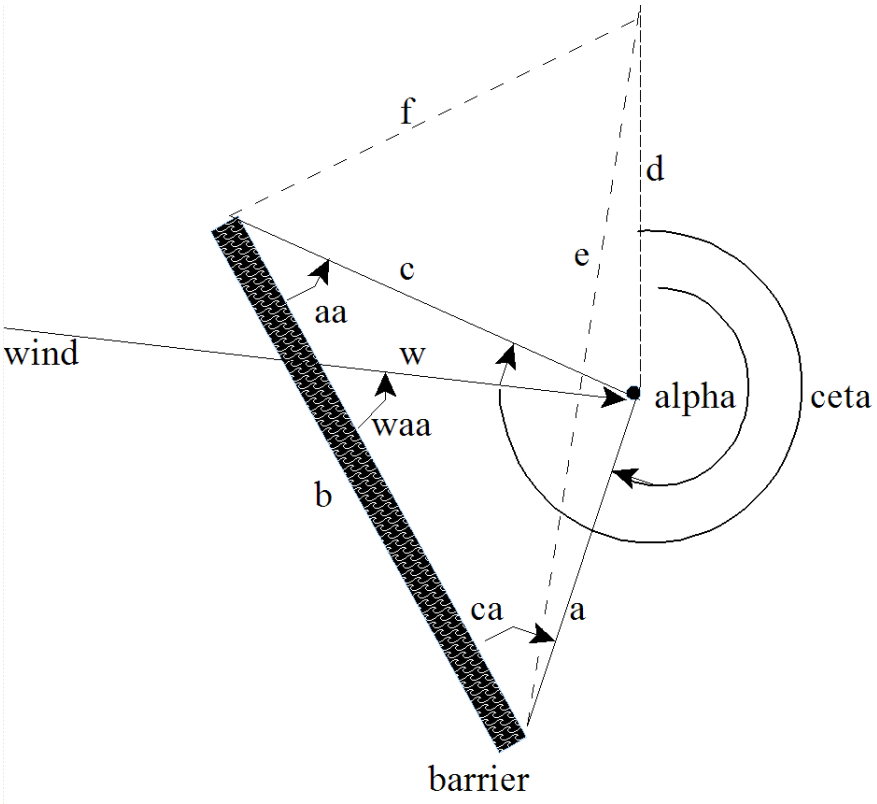

Fig. 12: Geometry of barrier effect calculations

cardinal directions and measured wind data can be at much higher resolution. It should be possible to use the provided wind direction for the calculation on a daily basis with little increase in computational effort. For each grid cell in the simulation region, calculations are used to determine the influence of each barrier in succession. The accuracy of the calculations could be increased by decreasing the grid cell size relative to the barrier height, but this can significantly increase computational effort.

A series of calculations were needed to determine the distance along the wind direction from the barrier to a grid cell, and their geometery is illustrated in Fig. 12. First, the coordinates (x_i, y_j) of the center of each cell are calculated. Next, distances (a and c) from the grid cell to the barrier ends and the barrier length (b) are determined. If a grid cell is on the barrier, i.e., $a + c = b$, then the fraction reduction in friction velocity is calculated directly.

For cells not on the barrier, angles at the barrier ends (aa and ca) are calculated. For example,

$$aa = cos^{-1} \frac{(b^2 + c^2 - a^2)}{2bc} \tag{56}$$

$$ca = cos^{-1} \frac{(a^2 + b^2 - c^2)}{2ab} \tag{57}$$

If the angles aa or ca are greater than 90 degrees, then the minimum distance between the cell center and the barrier (d_{min}) is the minimum of the lengths a or c. Otherwise d_{min} is calculated as in Fig. 12:

$$d_{min} = \frac{b * sin(aa) * sin(ca)}{sin(aa + ca)} \tag{58}$$

If d_{min} is less than 35 times the barrier height, additional calculations are used to determine the range of wind angles for which the barrier is upwind from the cell. To accomplish this task two angles (*alpha* and *ceta*, degrees from the line passing through the cell coordinates toward the positive y axis direction and lines a and c) were calculated. Next, for each relative wind direction that is between the angles *alpha* and *ceta*, i.e., the barrier is upwind of the grid cell, the distance between the barrier and the grid cell along the wind direction vector (w) is calculated by the sine rule as

$$w = \frac{a * sin(ca)}{sin(waa)} \tag{59}$$

where

waa is the angle between the barrier and the wind direction

The leeward distance w is converted to units of barrier heights, wz, and used in empirical equations developed using the data of Hagen et al. (1981), van Eimern et al. (1964), Raine and Stevenson (1977), and Hiesler and DeWalle (1988) to estimate the fraction of open field friction velocity (fu_*) in the sheltered area. (see Fig. 13) Note that an effective optical porosity of 1.0 can be used to give some barrier effect for minor of intermittent barriers. It should not be used when no barrier is present. The maximum porosity used in the development of the equations is 0.8, which should be considered the limit for equation validity. Also, in many areas, very porous barriers, such as barbed wire fencing, have the effect of capturing wind blown material (typically tumbleweeds) which greatly decrease their porosity.

$$fu_* = 1 - exp(-m * wz^2) + n * exp(-0.003(wz + s)^t) \tag{60}$$

where

fu_*= fraction of open field friction velocity

m, n, s, t = equation coefficients

The equation coefficients m, n, s, t are given by

$$m = 0.008 - 0.17pb + 0.17pb^{1.05} \tag{61}$$

$$n = 1.35exp(-0.5pb^{0.2}) \tag{62}$$

$$s = 10(1 - 0.5pb) \tag{63}$$

$$t = 3 - pb \tag{64}$$

where

pb = effective barrier porosity

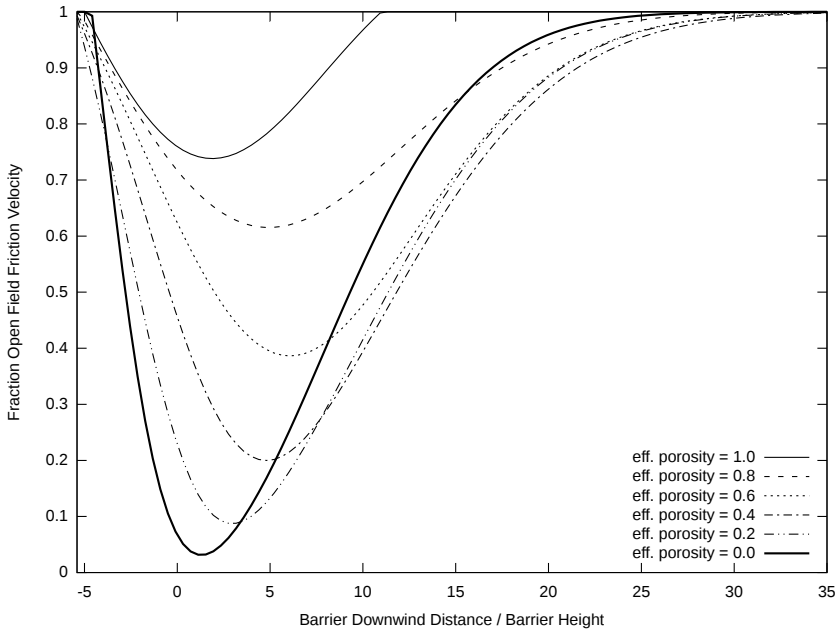

Fig. 13: Fraction of open field friction velocity as a function of distance downwind of barrier (negative distance is upwind of barrier) shown for different values of effective porosity.

Effective barrier porosity is found by adjusting optical barrier porosity as a function of barrier width (Fig. 14) using

$$pb = pbr + (1 - exp(-0.5xbr))^{0.3}(1 - pbr) \tag{65}$$

where

pbr = optical barrier porosity

xbr = normalized barrier width (barrier width divided by barrier height)

For all other grid cells which are not in the lee shelter region, but within 5 barrier heights from the barrier, a barrier influence was calculated using the minimum distance, wz, as a negative number in Eq. 60. When two or more barriers shelter the same area, the lowest fraction calculated for an individual barrier shelter is selected by the sub-model.

Knowing the influence of the barriers on each individual grid cell for the eight cardinal wind directions, when given a wind direction k, the friction velocity for each grid cell is found using:

$$U_*^{i,j} = U_* fu_*^{i,j,k} \tag{66}$$

where

$U_*^{i,j}$= the adjusted friction velocity for cell i, j with wind from direction k

$fu_*^{i,j,k}$= the reduction in wind velocity due to barriers for cell i, j from the wind direction k

Hills

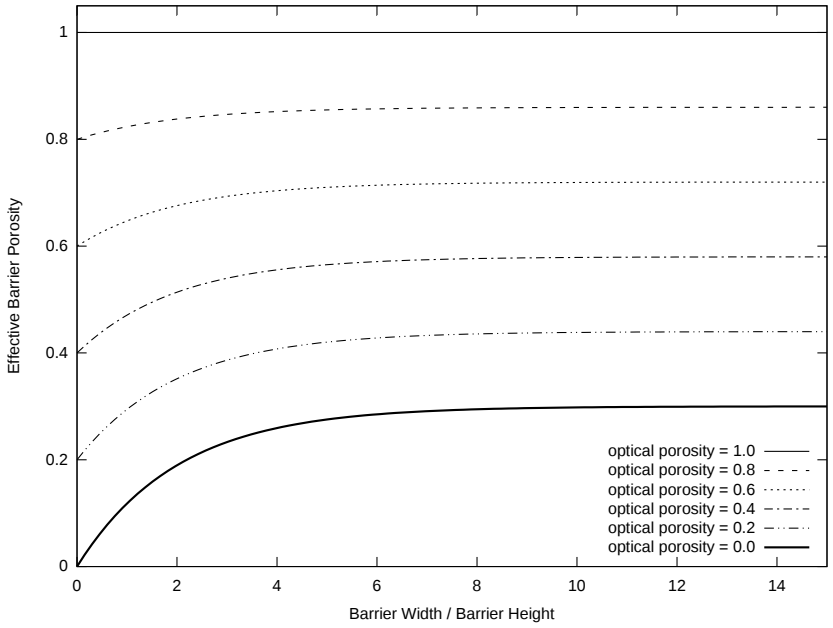

Fig. 14: Effective barrier porosity as a function of normalized barrier width.

Hills are not currently simulated in the current release of WEPS. However, it is anticipated that a speed up or slow down factor will be assigned to each cell based upon the wind direction as influenced by topography. Whether the necessary topographical data for each cell is provided externally, in an individual file, or natively as part of the field description has not been decided. Since WEATHER simulates a single wind direction for each day, only one set of factors would be used for each day with erosion at this time.

5.4 Threshold Friction Velocity

The velocity at which soil aggregates begin to saltate is defined as the static threshold friction velocity. Static threshold friction velocity is calculated in each grid cell as influenced by aggregate size and density, clod/crust cover, surface roughness, flat biomass cover, and surface soil wetness at noon.

As noted earlier, the fractional values of aggregated and crusted surface sum to one. However, to calculate the true fraction of bare, immobile surface, one must correct for both small aggregates and rock fraction, if present. Hence, the fraction of bare surface with immobile cover is :

$$SF_{cv} = \left[\left(1 - SF_{cr}\right)\left(1 - SF_{84}\right) + SF_{cr} - SF_{cr}SF_{los}\right]\left(1 - SV_{roc}\right) + SV_{roc} \tag{67}$$

where

SF_{cv}= soil fraction covered by clod, crust, and rock so it does not emit

SF_{cr}= soil fraction covered by crust, but excluding the fraction of rock-covered area

SF_{los}= soil fraction covered with loose, erodible soil on the crusted area

SV_{roc}= soil volume rock >2.0 mm. $\left(\frac{m^3}{m^3}\right)$

SF_{84}= soil fraction covered with aggregates <0.84 mm in diameter on the non-crusted area, but excluding the fraction of rock-covered area

The value of SF_{84} is calculated from the modified lognormal aggregate size distribution (Wagner and Ding 1994) input to ESM from other submodels as:

$$SF_{84} = \begin{cases} 0.5\left(1 + erf\left(\frac{\ln(SLT)}{\sqrt{2}\ln(SO_{ags})}\right)\right), & SL_{agx} > 0.84 \\ & and\, SL_{agn} < 0.84 \\ 1, & SL_{agx} \leq 0.84 \\ 0, & SL_{agn} \geq 0.84 \end{cases} \tag{68}$$

$$SLT = \frac{(0.84 - SL_{agn})(SL_{agx} - SL_{agn})}{(SL_{agx} - 0.84)SL_{agm}} \tag{69}$$

where

SL_{agn}= lower limit of size distribution (mm)

SL_{agx}= upper limit of size distribution (mm)

SL_{agm}= geometric mean of size distribution (mm)

SO_{ags}= geometric standard deviation of size distribution

To determine threshold friction velocities for bare soil surfaces, estimating equations were fitted to wind tunnel data (Hagen 1991b; Chepil and Woodruff 1963) to give (Fig. 15):

$$UB_{*ts} = 1.7 - 1.35\exp\left(-b1 - b2\left(SF_{cv}\right)^2\right) \tag{70}$$

$$b1 = -0.179 + 0.225\left(\ln\left(1 + Z0\right)\right)^{0.891} \tag{71}$$

$$b2 = 0.3 + 0.06Z0^{1.2} \tag{72}$$

where

UB_{*ts}= static threshold friction velocity of bare surface ($\frac{m}{s}$)

ZO= aerodynamic surface roughness (mm)

$b1$,$b2$= coefficients used in Eq. 70

Increased roughness increases form drag at the surface driving the increase in static threshold velocity. The dynamic threshold velocity is increased toward static threshold linearly in proportion to shelter area (SFA_{12}) (see Eq. 82).

If random flat biomass cover is present, the increase in static threshold friction velocity is (see Fig. 16)(Hagen 1996):

$$UC_{*ts} = \left(1 - \exp\left(-1.2BFF_{cv}\right)\right)\exp\left(-0.3SF_{cv}\right) \tag{73}$$

where

UC_{*ts}= change in static threshold friction velocity caused by flat biomass cover ($\frac{m}{s}$)

BFF_{cv}= biomass fraction of flat cover

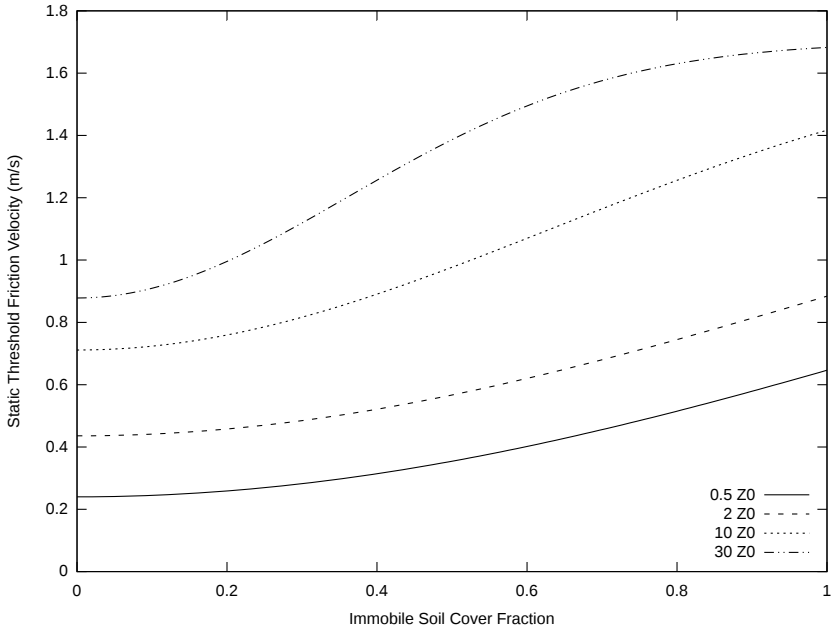

Fig. 15: Static threshold friction velocities for various levels of aerodynamic roughness and surface cover as predicted by Eq. 70.

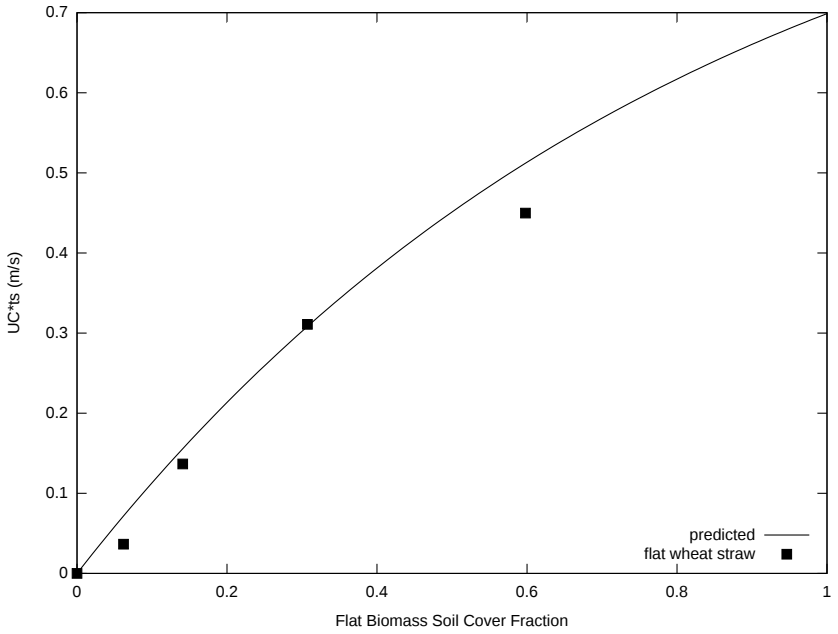

Fig. 16: Increase in static threshold friction velocity of erodible sand (0.29-0.42 mm); Flat wheat straw cover data from (Hagen 1996); Predicted is Eq. 73.

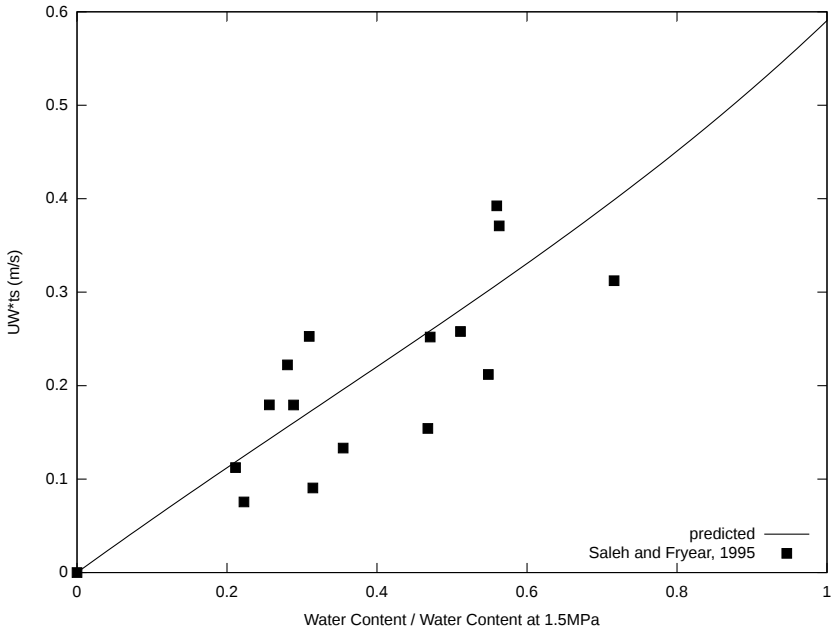

Fig. 17: Static threshold velocity change with water content relative to 1.5 Mpa water content; Predicted slope is Eq. 74 (Saleh and Fryrear 1995).

If the surface is wet, threshold velocity increases with the ratio of surface water content to the 15MPa water content (Fig. 17)(Saleh and Fryrear 1995) and is represented by:

$$UW_{*ts} = 0.58 \left(\exp\left(\frac{HRO_{wc}}{HR15_{wc}} \right) - 1 - 0.7 \left(\frac{HRO_{wc}}{HR15_{wc}} \right)^2 \right) \tag{74}$$

where

UW_{*ts}= increase in static threshold friction velocity from surface wetness $\left(\frac{m}{s}\right)$

$HR0_{wc}$= surface soil water content $\left(\frac{kg}{kg}\right)$

$HR15_{wc}$= surface soil water content at 1.5 MPa $\left(\frac{kg}{kg}\right)$

The equations for static threshold friction velocity were developed from wind tunnel studies where the erodible particles were quartz sand particles with a density of $2.65 \frac{Mg}{m^3}$. An adjustment for erodible soil, where the erodible particles are more likely to be aggregates is made. In WEPS, the aggregate density is set to $1.8 \frac{Mg}{m^3}$ while in SWEEP, the value can be specified. The adjustment equation is:

$$UD_{*ts} = 0.3 \left(\sqrt{\frac{SD_{agd}}{2.65}} - 1 \right) \tag{75}$$

where

UD_{*ts}= change in static threshold friction velocity from variable aggregate density $\left(\frac{m}{s}\right)$

SD_{agd}= aggregate density $\left(\frac{Mg}{m^3}\right)$

Finally, static threshold friction velocity adjusted for the non erodible soil fraction, flat biomass, surface wetness and aggregate density is:

$$U_{*ts} = UB_{*ts} + UC_{*ts} + UW_{*ts} + UD_{*ts} \tag{76}$$

where

U_{*ts}= adjusted surface static threshold friction velocity $\left(\frac{m}{s}\right)$

The static threshold friction velocity used in calculations of trapping and saltation/creep transport capacity equations (Bagnold 1943) is estimated by setting the surface cover fraction in Eq. 70 to a value of 0.4 and adding all the adjustments for flat biomass cover, surface wetness and aggregate density:

$$U_{*tp} = 1.7 - 1.35 \exp\left(-b1 - b2\left(0.4\right)^2\right) + UC_{*ts} + UW_{*ts} + UD_{*ts} \tag{77}$$

where

U_{*tp}= static threshold friction velocity for trapping and transport capacity $\left(\frac{m}{s}\right)$

Eq. 70 is also used to calculate a threshold friction velocity assuming dry conditions, no flat biomass cover, and the minimum aerodynamic roughness of $0.5mm$, which is used in the calculation of the maximum mobile soil fraction available for transport.

$$U_{*to} = 1.7 - 1.35 \exp\left(-b1^{ic} - b2^{ic}\left(SF_{cv}^{ic}\right)^2\right) \tag{78}$$

$$SF_{cv}^{ic} = \left(1 - SF_{84}^{ic}\right)\left(1 - SV_{roc}\right) + SV_{roc} \tag{79}$$

$$b1^{ic} = -0.179 + 0.225\left(\ln\left(1 + 0.5\right)\right)^{0.891} \tag{80}$$

$$b2^{ic} = 0.3 + 0.06\left(0.5\right)^{1.2} \tag{81}$$

where

U_{*to}= threshold friction velocity of a bare smooth surface with the erodible fraction of the surface before erosion occurs $\left(\frac{m}{s}\right)$

SF_{cv}^{ic}= bare surface cover fraction before erosion occurs ($SF_{84}^{ic} = SF_{84}$before erosion begins)

$b1^{ic}$= coefficient for smooth surface (aerodynamic roughness equals 0.5mm)

$b2^{ic}$= coefficient for smooth surface (aerodynamic roughness equals 0.5mm)

When the friction velocity exceeds the static threshold friction velocity and particles are in motion, the dynamic threshold friction velocity, or the friction velocity below which particle movement ceases is found by applying an adjustment dependent upon the fraction of the surface which is sheltered by random roughness elements.

$$U_{*t} = U_{*ts} - 0.05\left(1 - SFA_{12}\right) \tag{82}$$

where

SFA_{12}= total fraction of area sheltered with shelter angles >12 degrees

Likewise, the dynamic threshold for trapping and transport capacity is found using the same adjustment:

$$U_{*tt} = U_{*tp} - 0.05\left(1 - SFA_{12}\right) \tag{83}$$

5.5 Emission Parameters

As outlined in the theory section, the erosion process is modeled as the quasi-steady state conservation of mass using linked partial differential equations for three size classes of eroding soil. These are saltation/creep size (0.1 to 2.0 mm), suspension size (<0.1 mm), and PM_{10} size (<0.01 mm).

When the wind transport capacity exceeds the saltation/creep discharge, the net entrainment rate of loose surface soil into the airstream is directly proportional to the coefficient of emission, $C_{en}(m^{-1})$. A fraction of the emitted soil, SF_{SSen}, becomes part of the suspension discharge, and a fraction of the suspended soil from the emission, SF_{10en}, is PM_{10}. Estimations for the preceding three parameters are presented in this section.

For the complex surfaces simulated in ESM, auxiliary equations were developed to estimate C_{en}. The emission coefficient is calculated as a function of surface complexity as

$$C_{en} = C_{eno} R_{enb} R_{env} \tag{84}$$

where

C_{eno}= coefficient of emission for a bare, smooth, loose, erodible soil. A typical field value is about 0.06 $\left(\frac{1}{m}\right)$

R_{env}= emission ratio accounting for flat, random vegetation

R_{enb}= emission ratio accounting for immobile cover and surface roughness

The fractional emission factor to account for flat biomass cover is (Hagen 1996) (Fig. 18),

$$R_{env} = 0.075 + 0.934 \exp(-\frac{BFF_{cv}}{0.149}) \tag{85}$$

On rough surfaces, increasing the fraction of surface sheltered from direct saltation impacts by macro-roughness also reduces emission rates. A shelter angle at a point is defined as the largest angle above horizontal to the top of any upwind point. To predict the fraction of surface sheltered from saltation impacts, the random and ridge roughness can be used to estimate the sheltered area. The shelter angle distribution is described by a two parameter Weibull distribution; the two parameters are a scale factor and a shape factor (Potter, Zobeck, and Hagen 1990). The average shape factor measured over a range of roughness was about 0.77 (Potter and Zobeck 1990). The scale factor was related to the random roughness as

$$SAC_{rr} = 2.3\sqrt{SZ_{rr}} \tag{86}$$

where

SAC_{rr}= Weibull scale factor for random roughness, $(degrees)$

SZ_{rr}= random roughness (mm)(Allmaras et al. 1966)

The fraction horizontal area with shelter angles greater than 12 degrees caused by random roughness, SFA_{12rr}, is:

$$SFA_{12rr} = \exp\left(-\left(\frac{12}{SAC_{rr}}\right)^{0.77}\right) \tag{87}$$

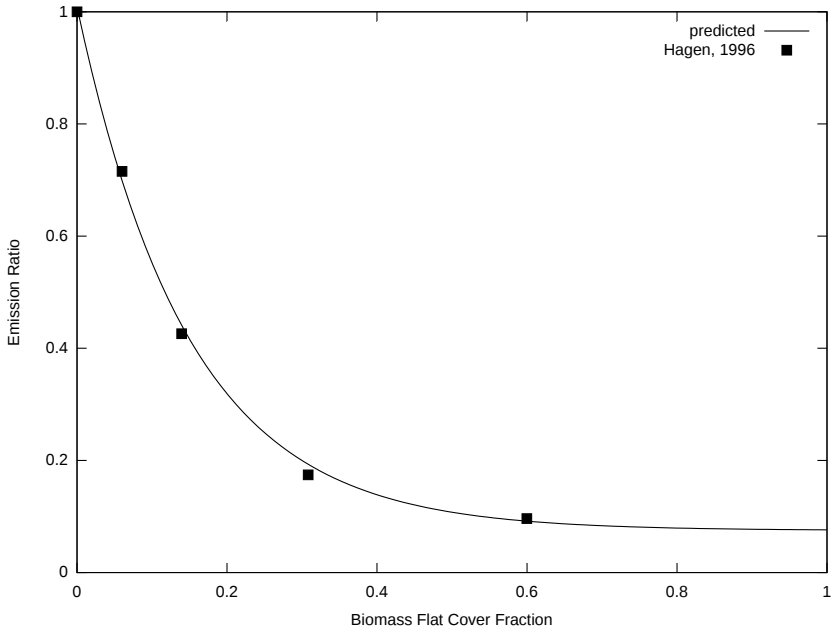

Fig. 18: Fractional emission factor of loose soil as function of increasing biomass flat cover; Predicted is Eq. 85 (Hagen 1996).

Similarly, the fraction of horizontal area sheltered by ridges, SFA12rg, can be calculated as (Potter and Zobeck 1990)

$$SAC_{rg} = \begin{cases} 65.4 \left(\dfrac{SZ_{rg}}{SXP_{rg}} \right)^{0.65}, & SZ_{rg} > 1 \, and \, SXP_{rg} > 10 \end{cases} \tag{88}$$

$$SFA_{12rg} = \begin{cases} \exp\left(- \left(\dfrac{12}{SAC_{rg}} \right)^{0.77} \right), & SZ_{rg} > 1 \, and \, SXP_{rg} > 10 \\ 0 & SZ_{rg} \leq 1 \, or \, SXP_{rg} \leq 10 \end{cases} \tag{89}$$

where

SAC_{rg}= Weibull scale factor for ridge shelter ($degrees$)

SZ_{rg}= ridge height (mm)

SXP_{rg}= ridge spacing parallel the wind direction (mm)

SFA_{12rg}= surface fraction of area with shelter angles >12 degrees for ridges

The area sheltered by ridges overlaps with the area sheltered by random roughness, so the resulting total fraction of area sheltered with shelter angles >12 degrees, SFA_{12}, is estimated as

$$SFA_{12} = (1 - SFA_{12rg}) \, SFA_{12rr} + SFA_{12rg} \tag{90}$$

On horizontal surfaces, immobile individual aggregates, rocks or pieces of crust tend to protrude slightly above the mobile surface and protect about 3 times their own horizontal

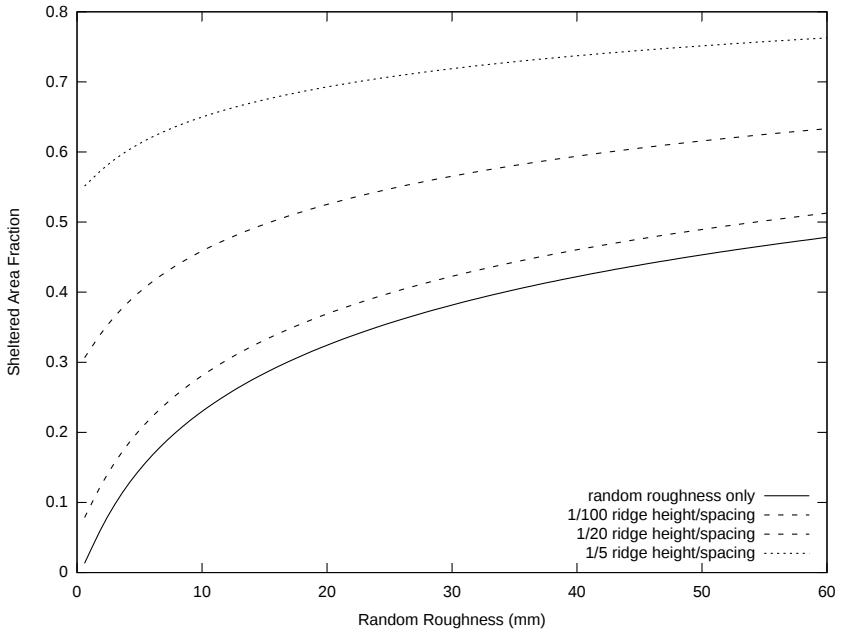

Fig. 19: Fraction of horizontal area with shelter angles >12 degrees as a function of random roughness and several ridge height spacing ratios as estimated by Eq. 90.

area from emissions. However, these small protrusions are usually part of the surface micro-roughness and not easily measured by conventional (pin) roughness meters. For comparison, sparse, flat, random biomass protects about 4 times its horizontal cover area from emissions as illustrated in Fig. 18. Similar to flat biomass, the areas protected by micro-roughness will begin to overlap as the cover of immobile aggregates, rock, and crust increases. Thus, the area not sheltered by either the micro-roughness or by the macro-roughness, as measured by roughness meters, ie. Eq. 67, is also used to estimate the emission ratio for bare soil. The emission from the surface is limited by the ability of the friction velocity to move soil particles. The mass of mobile soil particles, SM_{aglos}, is used to find the minimum mass of mobile soil particles at which emission will occur at the current friction velocity. The values are referenced to the bare smooth surface value at a friction velocity of 0.75 $\frac{m}{s}$, $SM_{aglosmx}$. The limited surface cover equation becomes:

$$SF_{cv}^{lim} = \begin{cases} [1 - SF_{cr}SF_{los}]\,(1 - SV_{roc}) + SV_{roc}, & SF_{84} \leq SF_{84mn} \\ SF_{cv}, & SF_{84} > SF_{84mn} \end{cases} \tag{91}$$

where the minimum mobile soil fraction for emission, SF_{84mn}, is found using the following:

$$SF_{84mn} = \max\left(0, \left(\frac{SM_{aglosmx} - SM_{aglos}}{SM_{aglosmx}SF_{84ic}\,(1.001 - SV_{roc})}\right)\right) \tag{92}$$

$$SM_{aglosmx} = \exp\left(2.708 - 7.603\left(\left(1 - SF_{84ic}\right)\left(1 - SV_{roc}\right)\right) + SV_{roc}\right) \tag{93}$$

$$SM_{aglos} = \max\left(0,\, SM_{aglosmx}\left(\frac{U_*^{i,j} - U_{*ts}}{0.75 - \min\left(U_{*to}, U_{*ts}\right)}\right)\right) \tag{94}$$

The bare soil emission ratio, R_{enb}, then is (Fig. 20):

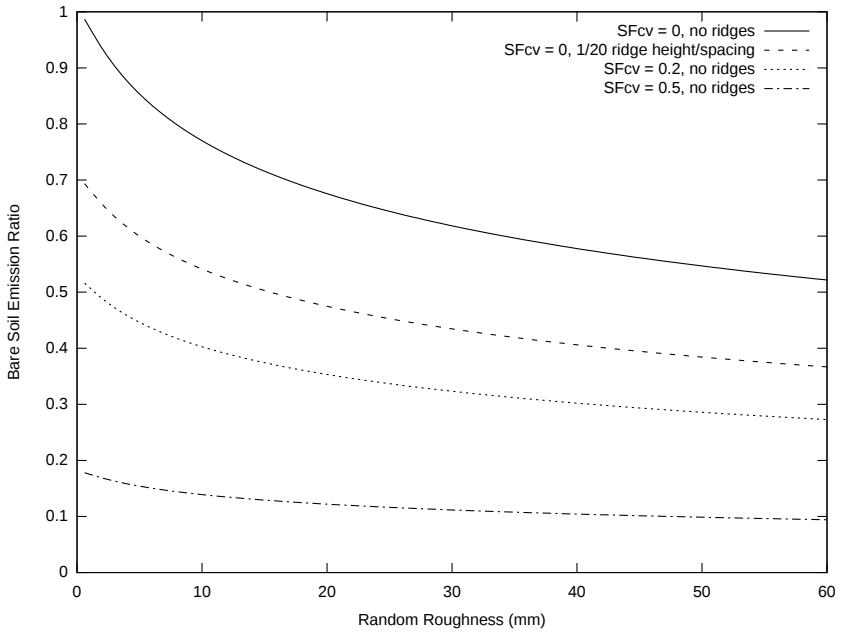

Fig. 20: Bare soil emission ratios predicted by Eq. 95 for ranges of immobile soil cover, a sample ridge, and random roughness.

$$R_{enb} = \left[-0.051 + 1.051 \exp\left(\frac{SF_{cv}^{lim}}{0.33050512}\right)\right](1 - SFA_{12}) \tag{95}$$

The soil fraction of suspension size in the emitted soil is estimated from the aggregate size distribution and the fraction of the surface that is crusted. As shown, the suspension portion is lower for the loose material on the crust.

$$SFss_{en} = \left(\frac{SF_{10}}{SF_{200} + 0.001}\right)(1 - 0.8SF_{cr}) \tag{96}$$

where

SF_{10}= soil fraction less than 0.10 mm diameter

SF_{200}= soil fraction less than 2.0 mm diameter

Fraction of PM_{10} in the emitted suspension-size aggregates is estimated as (Hagen, unpublished data)

$$SF10_{en} = 0.0067$$
$$+0.0000487\left[\min\left(300, \frac{SF_{sil}}{(SF_{cla} + 0.0001)^2}\right)\right] - 0.0000044WZ_{ypt} \tag{97}$$

where

SF_{sil}= suface soil fraction silt

SF_{cla}= surface soil fraction clay

WZ_{ypt}= average annual precipitation (mm)

5.6 Abrasion Parameters

The abrasion of immobile soil clods and crust by saltation/creep impacts creates additional erodible aggregates. The rate of creation of additional erodible aggregates depends upon the saltation/creep discharge, q_{sc} ($\frac{kg}{m \cdot s}$), the fractions of saltation/creep discharge impacting the clods and crust, F_{ani} , and the abrasion coefficients of the target clods and crust, C_{ani} ($\frac{1}{m}$). A fraction, $SFss_{an}$, of the erodible aggregates created by abrasion contribute to the suspension discharge, and a fraction, $SF10_{an}$, of the suspension-size aggregates created by abrasion are PM_{10}. Estimating equations for these parameters - F_{ani}, C_{ani}, $SFss_{an}$, and $SF10_{an}$ - are presented in this section.

The fraction of saltation/creep impact on both clods and crust that are not sheltered by either flat biomass or rock cover, F_{an}, is estimated as

$$F_{an} = \exp\left(-4BFF_{cv}\right) \exp\left(-3SV_{roc}\right) \tag{98}$$

where

BFF_{cv}= biomass fraction flat cover

SV_{roc}= soil volume of rock in surface layer $\left(\frac{m^3}{m^3}\right)$

The preceding equation assumes that both rock and flat biomass cover protrude slightly above the surrounding surface soil. The fraction of saltation/creep impacting on immobile aggregates, F_{anag}, is estimated as

$$F_{anag} = \left(1 - SF_{84}\right)\left(1 - SF_{cr}\right) F_{an} \tag{99}$$

where

SF_{84}= soil mass fraction of aggregates <0.84 mm diameter on aggregated surface

SF_{cr}= soil fraction of crust cover

The fraction of saltation/creep impacting on unprotected surface crust, F_{ancr}, is estimated as

$$F_{ancr} = SF_{cr}\left(1 - SF_{los}\right) F_{an} \tag{100}$$

where

SF_{cr}= surface fraction crust cover

SF_{los}= fraction of crust covered with loose, erodible soil

The abrasion coefficients for aggregates and crust are a function of their dry stabilities, and these were related in wind tunnel abrasion experiments (Fig. 21)(Hagen, Skidmore, and Saleh 1992) and curve fit to be

$$C_{anag} = \exp\left(-2.07 - 0.077\left(SE_{ags}\right)^{2.5} - 0.119\ln\left(SE_{ags}\right)\right) \tag{101}$$

where

C_{anag}= abrasion coefficient for aggregates $\left(\frac{1}{m}\right)$

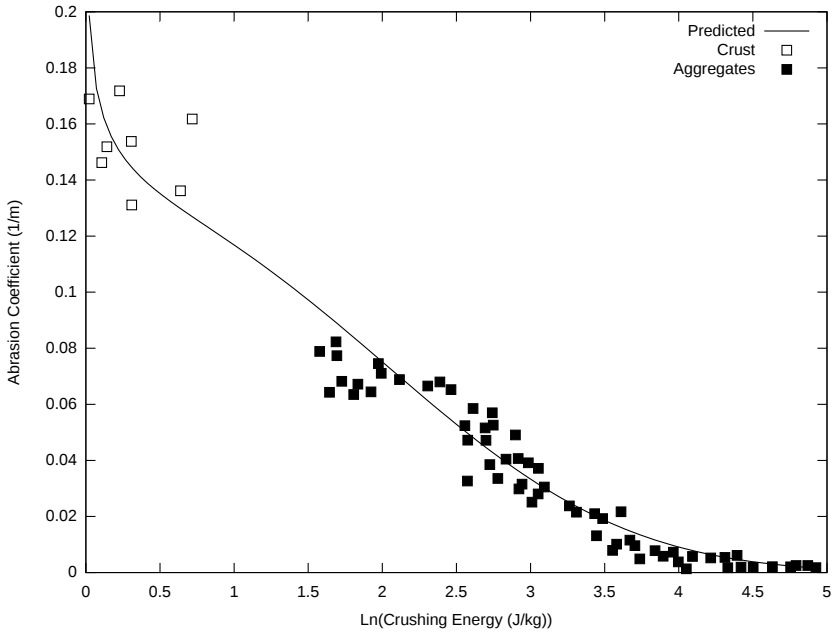

Fig. 21: Abrasion coefficients as a function of crushing energy; Predicted is Eq. 101 and 102; Data for soil crust and aggregates from (Hagen, Skidmore, and Saleh 1992).

SE_{ags}= dry stability of immobile aggregates $\left(\ln\left(\frac{J}{kg}\right)\right)$

and

$$C_{ancr} = \exp\left(-2.07 - 0.077\left(SE_{crs}\right)^{2.5} - 0.119\ln\left(SE_{crs}\right)\right) \tag{102}$$

where

C_{ancr}= abrasion coefficient for crust $\left(\frac{1}{m}\right)$

SE_{crs}= dry stability of crust $\left(\ln\left(\frac{J}{kg}\right)\right)$

An approximate estimate for crust abrasion coefficient used in ESM is to set it equal to the aggegated abrasion coefficient(Zobeck and Popham 1991).

$$C_{ancr} = C_{anag} \tag{103}$$

The soil fraction abraded from clods and crust that is of suspension size was determined experimentally (Mirzamostafa et al. 1998) and estimated as (Fig. 22)

$$SFss_{an} = \min\begin{pmatrix} 1 - \left(SF_{san} - SF_{vfs}\right),\ 0.4 - 4.83SF_{cla} + 27.18\left(SF_{cla}\right)^2 \\ -53.7\left(SF_{cla}\right)^3 + 42.25\left(SF_{cla}\right)^4 - 10.7\left(SF_{cla}\right)^5 \end{pmatrix} \tag{104}$$

where

SF_{cla}= surface soil fraction clay

SF_{san}= surface soil fraction sand

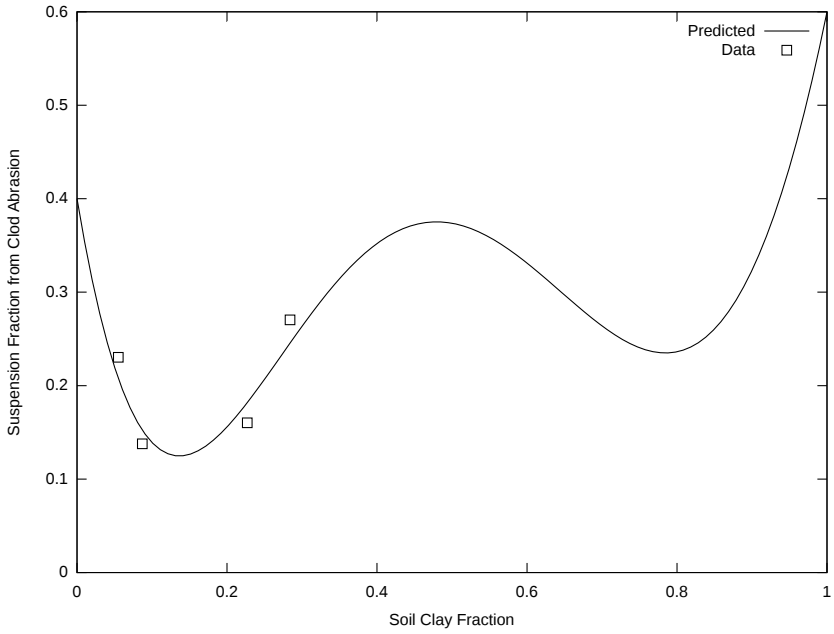

Fig. 22: Estimated soil fraction suspension-size in abraded soil as a function of clay content; Predicted is Eq. 104; Data is from (Mirzamostafa et al. 1998).

SF_{vfs}= surface soil fraction very fine sand

The fraction of PM_{10} in the abraded suspended soil is estimated as (Hagen, unpublished data)

$$SF10_{an} = 0.0116 + \frac{0.00025}{C_{anag} + 0.001} \tag{105}$$

5.7 Breakage Parameters

As saltation/creep-size aggregates are transported, they undergo multiple impacts and partial breakdown into suspension-size aggregates. Continuous movement of a single aggregate causes it to breakdown into primary particles, which may be a sand grain at its core. However, individual moving saltation/creep aggregates are frequently interchanged with similar aggregates on the surface, so the rate of breakdown can be estimated by a constant coefficient, C_{bk} $\left(\frac{1}{m}\right)$, as (Mirzamostafa 1996)

$$C_{bk} = 0.11 C_{anag} \left(1 - (SF_{san} - SF_{vfs})\right) \tag{106}$$

A fraction, $SF10_{bk}$, of the soil broken to suspension-size is PM_{10} and is estimated as (Hagen 2004)

$$\begin{aligned} SF10_{bk} &= 0.201 - 0.52 \ln\left(SF_{cla}\right) + 0.422 \left(\ln\left(SF_{cla}\right)\right)^2 \\ &-0.1395 \left(\ln\left(SF_{cla}\right)\right)^3 + 0.0156 \left(\ln\left(SF_{cla}\right)\right)^4 + 0.131 \exp\left(\frac{-WZ_{ypt}}{175.6}\right) \end{aligned} \tag{107}$$

where

$100 < WZ_{ypt} < 800$ annual precipitation(mm)

$0.017 < SF_{cla} < 0.42$ surface soil fraction clay

5.8 Trapping and Interception Parameters

There are three different cases of trapping and two of interception simulated in ESM. Examples of the first two cases can occur when a soil discharge approaches a wind barrier.

In the first case, the grid cell transport capacity, q_{en}, is zero, but the incoming saltation/creep, q_1 , is greater than zero. In this case, saltation/creep leaving the grid cell is set equal to zero and q_1 is the deposition rate for saltation/creep in the grid cell. In addition, the deposition of both the suspension and PM_{10} are simulated by simple exponential decay equations as

$$q_{ss} = q_{ss_1} \exp(-C_{dp}\,(\triangle X)) \tag{108}$$

$$q10 = q10_1 \exp(-C10_{dp}\,(\triangle X)) \tag{109}$$

where

1= subscript denoting values at upwind grid cell boundary

q_{ss}= suspension discharge $\left(\frac{kg}{m \cdot s}\right)$

$q10$= PM_{10} discharge $\left(\frac{kg}{m \cdot s}\right)$

C_{dp}= coefficient of deposition for suspension, estimated as 0.02 $\left(\frac{1}{m}\right)$

$C10_{dp}$= coefficient of deposition for PM_{10}, estimated as 0.001 $\left(\frac{1}{m}\right)$

In the second case, the incoming saltation/creep discharge, q_1, is greater than the transport capacity, q_{en}, in a grid cell. In this case, the saltation/creep discharge for the cell is set to q_{en}, while suspension and PM_{10} discharge are calculated using their usual estimating equations. The difference between q_1 and q_{en} is assigned as the deposition rate for saltation/creep in the grid cell.

In the third case, non-uniform surfaces, such as highly erodible tillage ridges, often emit more erodible saltation/creep than the wind can transport, and the excess emission is trapped in downwind furrows. Trapping is simulated when the surface is rough, i.e., ridge roughness >50 mm or random roughness >10 mm. The rate of trapping of the saltation/creep discharge depends on both the surface conditions and a trapping coefficient, $C_t\left(\frac{1}{m}\right)$. The trapping leads to the commonly-observed flattening of ridges and filling of furrows during erosion events.

An estimate for C_t , can be derived as follows: At sufficient distance downwind the saltation/creep discharge should approach the surface transport capacity. In this condition the emission flux, G_{en}, must equal the trapping flux, G_{tp}. Expanding and equating these values gives

$$(1 - SFss_{en})C_{en}(q_{en} - q) = C_t(q_{en} - q_{cp})\frac{q}{q_{en}},\ q_{en} \geq q_{cp} \tag{110}$$

Letting q approach q_{cp} and solving for C_t gives

$$C_t = (1 - SFss_{en})C_{en}\frac{q_{en}}{q_{cp}},\ q_{en} \geq q_{cp} \tag{111}$$

However, when $q_{en} \gg q_{cp}$, the transport capacity will be between them. Hence, a coefficient was substituted in the prior equation to give (with additional constraints specified):

$$C_t = \begin{cases} C_{tf}(1 - SFss_{en})C_{en}, & q_{en} \geq q_{cp}\, and\ (SZ_{rr} > 10\, or\, SZ_{rg} > 50) \\ 0, & q_{en} < q_{cp}\, or\ (SZ_{rr} \leq 10\, and\, SZ_{rg} \leq 50) \end{cases} \tag{112}$$

where

C_{tf}= empirical coefficient, with value about 1.2

Plant interception by standing biomass also decreases the discharge of saltation/creep. The deflection of saltation/creep by stems reduces their saltation jump along the wind direction and surface impact kinetic energy. These effects are estimated by an empirical coefficient of interception, $C_i\left(\frac{1}{m}\right)$, that is a function of biomass stem area, row orientation, and biomass height. The coefficient of interception is estimated as

$$C_i = \begin{cases} 0, & BZ < 0.001 \\ \left\{ \begin{array}{c} 0.005\left(1 - \exp\left(-\dfrac{0.5SAI}{BZ}\right)\right) \\ \sqrt{\dfrac{SX_{rg}}{SXP_{rg}}}\left(1 - \exp\left(-50BZ\right)\right) \end{array} \right\}, & \begin{array}{l} BZ \geq 0.001 \\ SX_{rg} > 10 \end{array} \\ \left\{ \begin{array}{c} 0.005\left(1 - \exp\left(-\dfrac{0.5SAI}{BZ}\right)\right) \\ \left(1 - \exp\left(-50BZ\right)\right) \end{array} \right\}, & \begin{array}{l} BZ \geq 0.001 \\ SX_{rg} \leq 10 \end{array} \end{cases} \tag{113}$$

where

SAI= stem silhouette area index

BZ= biomass height

SX_{rg}= ridge spacing (mm)

SXP_{rg}= ridge spacing parallel the wind direction

Standing biomass leaves and stems also intercept a portion of the suspension-size aggregates. In this case, we assumed the suspended soil from upwind was moving above the biomass so only part of the suspension-size soil moving from below to above the biomass in a grid cell was intercepted. The fraction of the vertical suspension flux intercepted (Css_i) is estimated as

$$Css_i = 0.1SAI \tag{114}$$

6 Update of Surface Conditions during Wind Erosion

Changes to the soil surface in response to loss or deposition at various downwind field locations are rarely considered in wind erosion models. However, it appears necessary to update surface conditions during significant erosion events to account for depletion of the reservoir of mobile soil on short fields, and to simulate the increased erodibility typically observed on downwind regions in long fields. In general, few measurements are available to validate the simulated response of field surfaces to erosion. Hence, simple equations based on mass balance in the surface layer were developed to simulate changes in the area represented by each grid cell.

6.1 Surface Update Intervals (time steps)

In WEPS 1.0, hourly simulated or measured wind speeds are used as model inputs. Other intervals for measured wind speeds can be used as inputs to both WEPS and SWEEP. Accounting routines assume that the intervals used evenly divide one hour and that the same interval is used for the entire simulation.

To minimize model run time, a variable update time interval was implemented. The needed surface update interval depends on the erosion rate, but that is unknown before a simulation is made. Hence, when each new wind speed is input, a relative erosive wind energy $\left(ENG_e, \frac{m^3}{s^3}\right)$ is calculated for the most erosive grid cell during the previous time step as

$$ENG_e = (U_{*e})^2 (U_{*e} - U_{*te}) \tag{115}$$

where

U_{*e}= estimated friction velocity found to be 0.06 of the 10 meter wind velocity for this time period

U_{*te}= estimated threshold friction velocity found to be $\frac{U_{*e}}{rut}$

rut = ratio of friction velocity for this time period to daily initial threshold friction velocity

The number of surface updates for each of the wind speeds input during 24 hours is

$$N_t = \max\left(1, \frac{96}{N_{tstep}}\right) \tag{116}$$

$$N = \max\left(1, (0.5 + 4.6 ENG_e) N_t\right) \tag{117}$$

where

N_{tstep}= number of wind speed intervals input in 24 hour time period

N_t = minimum number of time steps required for surface updating for each wind speed interval

N = number of time steps for surface updating for each wind speed interval

Surface update intervals as a function of relative erosive wind energy then become:

$$\triangle t = \frac{86400}{N \cdot N_{tstep}} \tag{118}$$

which is illustrated in Fig. 23 where

$\triangle t$ = surface update time interval (s)

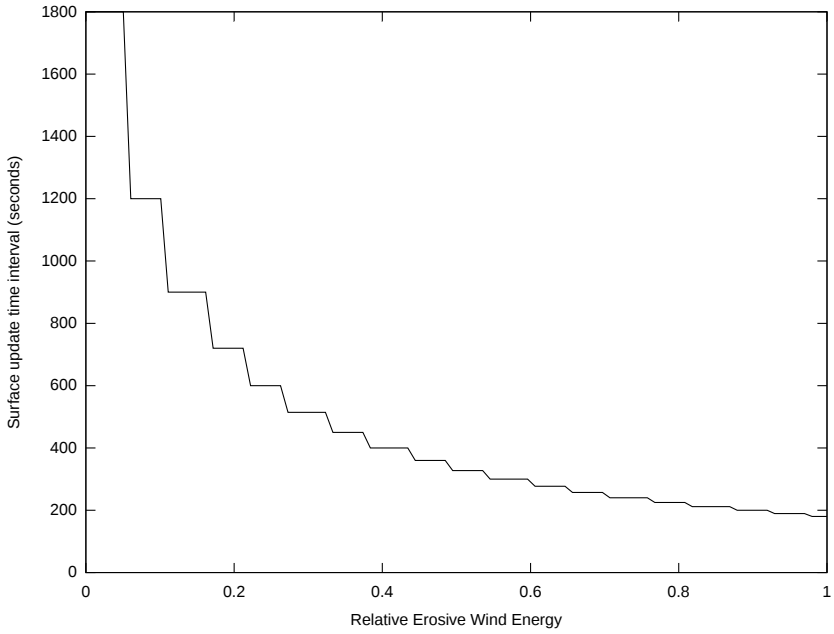

Fig. 23: Surface update time interval based on relative erosive wind energy.

6.2 Change in Mobile Surface Soil

Two reservoirs of mobile soil may be present at the soil surface. These include mobile soil on a consolidated surface, hereafter called crusted, and mobile soil among the rock and immobile aggregates. Because these reservoirs differ in their response to erosion, they are updated separately. Written in general form, the equation for the net addition (+) or loss (-) of mobile aggregates during a time interval ($\triangle t$) over a field length segment ($x_2 - x_1$) from a reservoir is estimated as

$$dmt_{los} = dmt + \left[\sum_{i=1}^{2} (F_{an_i} C_{an_i})\right] q_1 \triangle t \tag{119}$$

$$dmt = \left(\frac{-(q_2 - q_1) - (qss_2 - qss_1)}{x_2 - x_1}\right) \triangle t \tag{120}$$

where

dmt_{los} = net change in mobile soil surface aggregates during time interval $\triangle t$ $\left(\frac{kg}{m^2}\right)$

dmt = net gain(+) or loss(-) of soil from grid in time interval$\triangle t$ $(\mathrm{kg/m^2})$

The first term in Eq. 119 represents loss or gain by erosion and the second term represents creation of new mobile aggregates by the abrasion process.

6.3 Update of Crusted Surface

Undisturbed, crusted soil surfaces have high threshold wind speeds and are generally stable, unless abraded by mobile soil aggregates. In WEPS, the crust is simulated as a triangular shape (Fig. 24). Uniform abrasion of this crust shape continually exposes an increasing area of aggregated soil at the surface. The simple triangular shape was selected because

there are spatial variations in crust thickness and resistance to abrasion interacting with preferential zones for abrader impact caused by the surface micro-topography within each grid cell that is, nevertheless, assumed to be homogeneous.

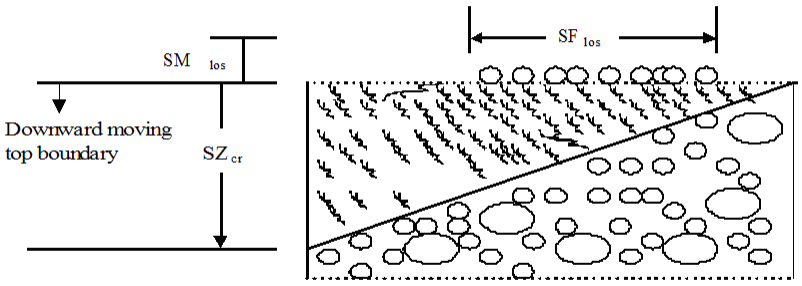

Figure 2- Schematic of triangular-shaped crust on soil surface layer subject to soil loss by wind erosion.

Fig. 24: Schematic of triangular-shaped crust on soil surface layer subject to soil loss by wind erosion.

The deflatable mass of mobile soil on the crusted surface, SM_{los0}, is not dependent on the magnitude of the friction velocity above threshold. All of the reservoir is available. If the reservoir of mobile soil on the crust cannot fully supply the simulated soil loss ($-dmt_{los} > SM_{los0}$), the additional soil loss, fdm, is removed from the remaining reservoir of mobile soil among rocks and immobile aggregates.

$$\begin{gathered} \left\{ \begin{array}{c} SM_{los} = SM_{los0} + dmt_{los} \\ fdm = 0 \end{array} \right\}, -dmt_{los} \leq SM_{los0} \\ \left\{ \begin{array}{c} SM_{los} = 0 \\ fdm = (SM_{los0} + dmt_{los}) \dfrac{SF_{cr}}{1.0001 - SF_{cr}} \end{array} \right\}, -dmt_{los} > SM_{los0} \end{gathered} \tag{121}$$

where

SM_{los} = mobile soil aggregates per unit area of the crusted surface $\left(\frac{kg}{m^2}\right)$

SM_{los0} = value of SM_{los}at prior time step $\left(\frac{kg}{m^2}\right)$

fdm = additional net change in mobile soil surface aggregates for aggregated surface during time interval $\triangle t$ $\left(\frac{kg}{m^2}\right)$

Updated values of the mobile aggregate mass on the crusted surface are used to update the fraction of mobile crust cover. The layer thickness of mobile aggregate deposits tends to increase with surface roughness. Hence, the coefficient CR_{los} reduces mobile cover as surface roughness increases.

$$SF_{los} = (1 - \exp(3.5\, SM_{los}^{1.5}))CR_{los} \tag{122}$$

$$CR_{los} = \exp(-0.8\sqrt{SZ}) \tag{123}$$

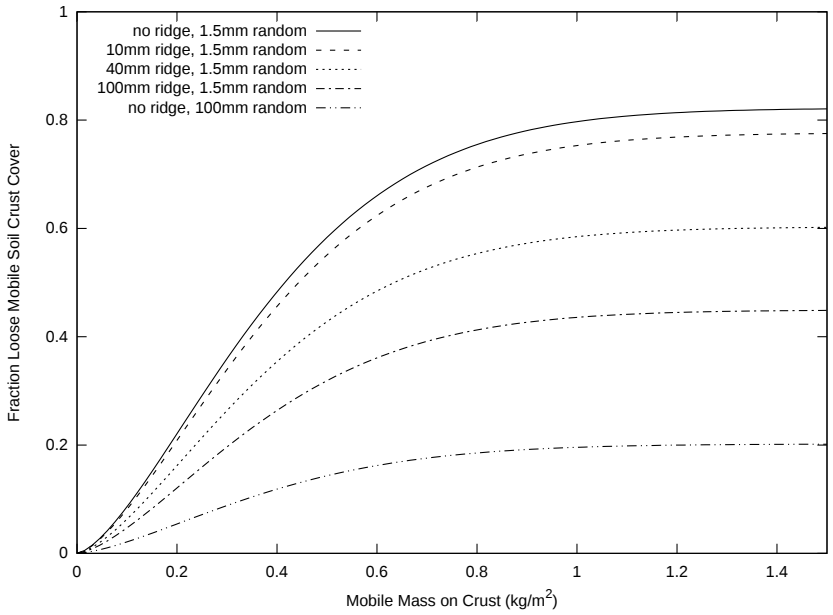

Fig. 25: Loose, mobile cover of aggregates on crust as a function of mobile mass for a range of ridge heights

$$SZ = \max(SZ_{rg}, 4\,SZ_{rr}) \tag{124}$$

where

CR_{los}= roughness dependent fraction of mobile crust cover reduction coefficient

SZ_{rg}= ridge height (mm)

SZ_{rr}= random roughness (mm)

Mobile aggregate cover on a crusted surface as a function of mobile mass with various ridge height levels is illustrated in Fig. 25.

If fraction crust cover is >0.01, crust thickness is reduced by abrasion on the crust and is simulated as

$$SZ_{cr} = SZ_{cr0} - \frac{F_{ancr} C_{ancr} q_1}{1.4 SF_{cr}} \triangle t \tag{125}$$

where

SZ_{cr}= crust thickness (mm)

SZ_{cr0}= crust thickness at prior time step (mm)

F_{ancr}= updated value from Eq. 100 using updated SF_{los}

Finally, crust cover is updated in proportion to crust thickness as

$$SF_{cr} = SF_{cr0} \frac{SZ_{cr}}{SZ_{cr0}} \tag{126}$$

where

SF_{cr0}= is crust cover fraction at prior time step

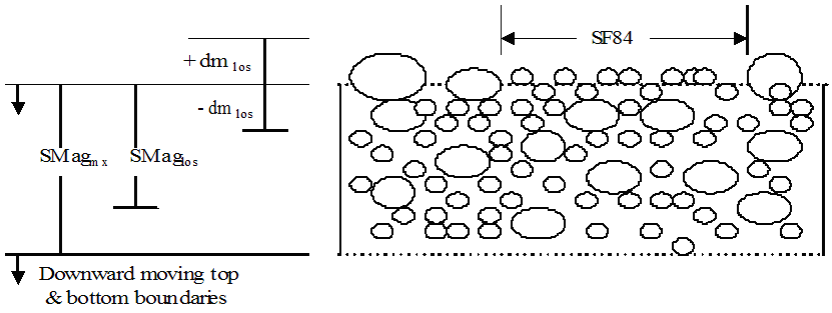

Fig. 26: Schematic of aggregated soil surface layer subject to soil loss by wind erosion.

6.4 Update of Aggregated Surface

On aggregated surfaces some of the mobile material is typically sheltered by micro-roughness of the immobile aggregates. Hence the reservoir of mobile material available for deflation varies with friction velocity. The maximum mass of mobile soil that could be removed under a high friction velocity is $SMag_{mx}$, while removable soil under a lowered friction velocity is $SMag_{los}$ as illustrated in Fig. 26. The mobile aggregate cover fraction on the aggregated surface is $SF84$. The aggregate mixture is assumed to be uniform with depth. Hence, as abrasion lowers the soil surface, the top and bottom boundaries move downward so that $SMag_{mx}$ remains constant. The net mass of mobile soil removed(-) or added (+) to the reservoir is dm_{los}.

To simulate the aggregated surface, the cumulative change of mass of mobile material is updated as

$$dm_{los} = dm_{los0} + dmt_{los} + fdm \tag{127}$$

where

dm_{los}= cumulative mobile soil loss or gain on aggregated surface $\left(\frac{kg}{m^2}\right)$

dm_{los0}= value of dm_{los} at prior time step $\left(\frac{kg}{m^2}\right)$

When $dm_{los} < 0$, mobile soil is removed from the initial reservoir among the immobile aggregates. Based on limited wind tunnel measurements, empirical relationships were developed to estimate the mass of mobile aggregates that could be removed from a flat, bare, aggregated surface for a range of friction velocities as illustrated in Fig. 27.

The maximum removable mass in the mobile reservoir was estimated at a friction velocity (U_*) of 0.75 m/s for a bare, smooth, aggregated surface as

$$SM_{aglosmx} = \exp(2.708 - 7.603((1 - SF84_{ic})(1 - SVroc_{ic}) + SVroc_{ic}) \tag{128}$$

The total soil mass in the reservoir is then estimated as

$$SM_{tot} = \frac{SM_{aglosmx}}{SF84_{ic}(1.001 - SVroc_{ic})} \tag{129}$$

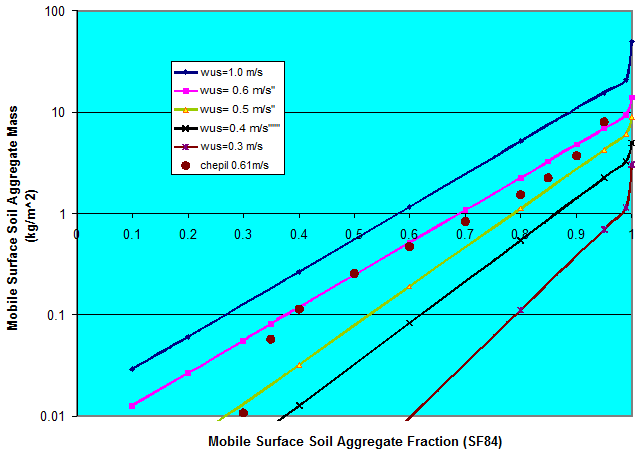

Fig. 27: Mass of mobile aggregates that can be removed from flat, bare aggregated surface with various initial mass fractions of mobile aggregates (SF84) for a range of friction velocities without abrasion. Data from Chepil (1951)

The maximum reservoir is reduced by roughness, residue cover, and wetness to estimate the available reservoir at the current friction velocity as

$$SM_{aglos} = \max\left(0,\, SM_{aglosmx}\frac{U_* - U_{*t}}{0.75 - U_{*to}}\right) \tag{130}$$

where

U_{*to}= threshold friction velocity for bare, aggregated, smooth soil ($\frac{m}{s}$)

When the soil removal from the reservoir with the current friction velocity equals SM_{aglos}, erosion is stopped, and the mobile soil fraction (SF_{84mn}) still remaining in the maximum mobile soil reservoir is

$$SF_{84mn} = \frac{SM_{aglosmx} - SM_{aglos}}{SM_{tot}} \tag{131}$$

When there is net soil mass deposition ($dm_{los} \geq 0$), the immobile surface aggregates can become slowly buried by the addition of mobile soil to the initial reservoir. In this case, the surface fraction of mobile aggregates is adjusted upward. For both loss and deposition, SF_{84} is updated as

$$SF_{84} = \begin{cases} \dfrac{SM_{aglosmx} + dm_{los}}{SM_{tot}}, & dm_{los} < 0 \\ \dfrac{SM_{aglosmx} + dm_{los}}{SM_{tot} + dm_{los}}, & dm_{los} \geq 0 \end{cases} \tag{132}$$

6.5 Update of Soil Fraction <2.0 mm Diameter

The soil fraction <2.0 mm diameter (SF_{200}) is estimated from the values of the soil fraction <0.84 mm diameter (SF_{84}) as

$$SF_{200} = (2 - SF_{84})\, SF_{84} \tag{133}$$

6.6 Update of Soil Fraction <0.10 mm Diameter

When soil loss is occurring (dm_{los} <0.0), SF_{10} is updated in proportion to the changes in SF_{84}. When there is mobile soil gain at the soil surface ($dm_{los} \geq 0$), the suspension-size aggregates less than 0.10 mm diameter (SF_{10}) tend to be sorted out of the depositing soil. Hence, the estimate is

$$SF_{10} = \begin{cases} SF_{10ic}\dfrac{SF_{84}}{SF_{84ic}}, & dm_{los} < 0 \\ \dfrac{SF_{10ic}SM_{tot}}{SM_{tot} + dm_{los}}, & dm_{los} \geq 0 \end{cases} \tag{134}$$

where

SF_{10ic}= is the SF_{10} initial condition at the beginning of the erosion event

SF_{84ic}= is the SF_{84} initial condition at the beginning of the erosion event

6.7 Update of Surface Rock Volume

The rocks (>2.0 mm diameter) are assumed to be mixed with the soil and have a uniform vertical distribution. If an initial desert pavement is present, the surface is generally assumed to be stable. Surface rock volume increases or decreases in proportion to the deflation or deposition from the surface area that is not covered by rock and is estimated to slowly change by the equation

$$SV_{roc} = \min\left\{1,\, \max\left\{0,\, SV_{roc0} - \left(\frac{1 - SV_{roc0}}{1 - SV_{rocic}}\right)\left(\frac{7.5dmt}{1200\,(1.001 - SV_{rocic})}\right)\right\}\right\} \tag{135}$$

where

SV_{roc} = soil rock volume$\left(\frac{m^3}{m^3}\right)$

SV_{roc0} = soil rock volume at prior time-step$\left(\frac{m^3}{m^3}\right)$

SV_{rocic} = soil rock volume at beginning of erosion event$\left(\frac{m^3}{m^3}\right)$

6.8 Update Surface Roughness

Roughness elements consist of random roughness and, if present, oriented roughness such as tillage ridges. The first step in updating roughness is estimating the effects of changes in loose soil depth generated by the various erosion processes. Trial relationships were developed based on qualitative criterion for testing. When the soil surface has roughness elements that actively trap saltation-size aggregates ($C_t > 0$) and net deposition of mobile soil in sheltered areas ($dmt_{los} > 0$), roughness height decreases. When saltation trapping occurs ($C_t > 0$), but with a net loss from both sheltered and unsheltered areas ($dmt_{los} \leq 0$), roughness height decreases, but more slowly. When no saltation trapping is occurring ($C_t = 0$), i.e the soil surface is relatively smooth, a net deposition increase over much of the area ($dmt_{los} > 0$) decreases roughness height. Finally, when no saltation trapping is

occurring ($C_t = 0$), the net loss of loose surface material ($dmt_{los} \leq 0$) increases roughness. Quantitative research is needed to refine these relationships.

$$SZ_v = \begin{cases} \dfrac{-2.0 dmt_{los}}{1.2}, & C_t > 0 \, and \, dmt_{los} > 0 \\ \dfrac{dmt_{los}}{1.2}, & C_t > 0 \, and \, dmt_{los} \leq 0 \\ \dfrac{-dmt_{los}}{1.2}, & C_t = 0 \, and \, dmt_{los} > 0 \\ \dfrac{0.5 dmt_{los}}{1.2}, & C_t = 0 \, and \, dmt_{los} \leq 0 \end{cases} \tag{136}$$

where

SZ_v= change is roughness height caused by deposition or emission for time step $\triangle t$ (mm)

The change in roughness height caused by abrasion of immobile clods and crust is

$$SZ_{an} = \frac{-2.0 \left[\sum_{i=1}^{2} (F_{an_i} C_{an_i}) \right] q_1 \triangle t}{1.4} \tag{137}$$

where

SZ_{an}= change is roughness height caused by abrasion for time step $\triangle t$ (mm)

Total roughness height change is then expressed as, SZ_t (mm) is

$$SZ_t = SZ_v + SZ_{an} \tag{138}$$

where

SZ_t= total change is roughness height for time step $\triangle t$ (mm)

Ridge height is updated as

$$SZ_{rg} = \max \{0, SZ_{rg0} + SZ_t\} \tag{139}$$

where

SZ_{rg}= ridge height (mm)

SZ_{rg0}= ridge height at prior time-step (mm)

Random roughness is updated as

$$SZ_{rr} = \max \left\{ 1.5, SZ_{rr0} \frac{SZ_t}{4.0} \right\} \tag{140}$$

where

SZ_{rr}= random roughness (mm)

SZ_{rr0}= random roughness at prior time-step (mm)

7 Output from Erosion to Files

The submodel outputs include estimates of both total soil loss from the simulation region as well as components of the soil loss moving across each field boundary. These components are saltation/creep (>0.10 mm diameter) and suspended soil (<0.10 mm diameter). The mass of particles less than 10 microns in aerodynamic diameter (PM_{10}) in the suspended soil also is predicted. Files of time-varying emissions for use as source terms in dust diffusion and transport models can also be output. To compare simulation results to measured erosion data, input files of measured weather can be used in place of the simulated weather.

When called from the full WEPS model, the summary results of total erosion, creep-/saltation, suspension, and PM_{10} from each erosion day are provided to routines which summarize erosion results by period over all years and by year. In addition, the daily erosion mass across the four field side boundaries are also provided for summarization.

When called from the SWEEP model, output files are created for daily total erosion amounts for all components (*.erod); hourly total erosion amounts for all components (*.emit); field grid cell boundary total erosion amounts and field grid cell total erosion amounts for all components (*.egrd); and detailed conditions and erosion amounts for each grid cell by time step (*.sgrd).

```
7.977219      1.903312      6.073907      0.232969  test.in
```

Fig. 28: Example *.erod file showing total erosion results. Values are total erosion, creep-/saltation, suspension, and the PM_{10}portion of suspension for a single day erosion event in $\frac{kg}{m^2}$.

SBEMIT output

Date of run: Feb 08, 2010 15:02:31

yr	mo	day	hr	ws	emission (kg m-2 s-1) total	salt/creep	susp	PM10
1	1	1	1.000	1.60	0.00000000	0.00000000	0.00000000	0.00000000
1	1	1	2.000	0.00	0.00000000	0.00000000	0.00000000	0.00000000
1	1	1	3.000	0.00	0.00000000	0.00000000	0.00000000	0.00000000
1	1	1	4.000	0.00	0.00000000	0.00000000	0.00000000	0.00000000
1	1	1	5.000	0.00	0.00000000	0.00000000	0.00000000	0.00000000
1	1	1	6.000	1.00	0.00000000	0.00000000	0.00000000	0.00000000
1	1	1	7.000	2.10	0.00000000	0.00000000	0.00000000	0.00000000
1	1	1	8.000	2.80	0.00000000	0.00000000	0.00000000	0.00000000
1	1	1	9.000	3.30	0.00000000	0.00000000	0.00000000	0.00000000
1	1	1	10.000	4.00	0.00000000	0.00000000	0.00000000	0.00000000
1	1	1	11.000	5.60	0.00000000	0.00000000	0.00000000	0.00000000
1	1	1	12.000	6.60	0.00000000	0.00000000	0.00000000	0.00000000
1	1	1	13.000	12.70	0.00000000	0.00000000	0.00000000	0.00000000
1	1	1	14.000	14.50	0.00000000	0.00000000	0.00000000	0.00000000
1	1	1	15.000	19.40	0.00000000	0.00000000	0.00000000	0.00000000
1	1	1	16.000	27.80	0.00221589	0.00052870	0.00168720	0.00006471
1	1	1	17.000	14.80	0.00000000	0.00000000	0.00000000	0.00000000
1	1	1	18.000	14.30	0.00000000	0.00000000	0.00000000	0.00000000
1	1	1	19.000	7.90	0.00000000	0.00000000	0.00000000	0.00000000
1	1	1	20.000	5.90	0.00000000	0.00000000	0.00000000	0.00000000
1	1	1	21.000	4.50	0.00000000	0.00000000	0.00000000	0.00000000
1	1	1	22.000	3.60	0.00000000	0.00000000	0.00000000	0.00000000
1	1	1	23.000	3.00	0.00000000	0.00000000	0.00000000	0.00000000
1	1	1	24.000	2.40	0.00000000	0.00000000	0.00000000	0.00000000

Fig. 29: Example *.emit file listing showing hourly wind speed (ws), and emissions for each hour.

```
OUTPUT FROM ERODOUT.FOR
Date of run: Feb 08, 2010 15:02:31
<field dimensions>
      0.00      0.00      0.00    705.61    705.61
</field dimensions>
Total grid size: ( 31 , 31 )   Inner grid size: ( 29 , 29 )

  Passing Border Grid Cells - Total  egt+egtss(kg/m)
  top(i=1,imax-1,j=jmax) bottom(i=1,imax-1,j=0) right(i=imax,j=1,jmax-1) left(i=0, j=1,jmax-1)
     73.9373    308.7460     ...    4701.3433   4795.3286
      0.0000      0.0000     ...       0.0000      0.0000
     73.9308    308.7312     ...    4701.3125   4795.3008
      0.0000      0.0000     ...       0.0000      0.0000

  Passing Border Grid Cells - Salt/Creep   egt(kg/m)
  top(i=1,imax-1,j=jmax) bottom(i=1,imax-1,j=0) right(i=imax,j=1,jmax-1) left(i=0, j=1,jmax-1)
     55.4283    213.7831     ...     736.4492    736.4492
      0.0000      0.0000     ...       0.0000      0.0000
     55.4235    213.7734     ...     736.4448    736.4448
      0.0000      0.0000     ...       0.0000      0.0000

  Passing Border Grid Cells - Suspension egtss(kg/m)
  top(i=1,imax-1,j=jmax) bottom(i=1,imax-1,j=0) right(i=imax,j=1,jmax-1) left(i=0, j=1,jmax-1)
     18.5090     94.9629     ...    3964.8940   4058.8796
      0.0000      0.0000     ...       0.0000      0.0000
     18.5072     94.9578     ...    3964.8679   4058.8560
      0.0000      0.0000     ...       0.0000      0.0000

  Passing Border Grid Cells - PM10       egt10(kg/m)
  top(i=1,imax-1,j=jmax) bottom(i=1,imax-1,j=0) right(i=imax,j=1,jmax-1) left(i=0,j=1,jmax-1)
    0.492453    2.614820     ...  154.967499  158.734940
    0.000000    0.000000     ...    0.000000    0.000000
    0.492406    2.614674     ...  154.966537  158.734009
    0.000000    0.000000     ...    0.000000    0.000000

<grid data> | |Total Soil Loss|soil loss|(kg/m^2)
     -3.4172    -10.5349     ...      -7.7256     -7.7256
     -2.9983     -9.9498     ...      -7.7256     -7.7256
       .           .         ...        .           .
       .           .         ...        .           .
       .           .         ...        .           .
     -0.2785     -0.4988     ...      -9.9495    -10.5346
     -0.2074     -0.2785     ...      -2.9980     -3.4170
</grid data>

<grid data> | |Saltation/Creep Soil Loss|salt/creep soil loss|(kg/m^2)
     -2.5596     -7.1146     ...       0.0000      0.0000
     -2.2505     -6.7303     ...       0.0000      0.0000
       .           .         ...        .           .
       .           .         ...        .           .
       .           .         ...        .           .
     -0.2146     -0.3720     ...      -6.7301     -7.1144
     -0.1643     -0.2146     ...      -2.2503     -2.5594
</grid data>

<grid data> | |Suspension Soil Loss|suspension soil loss|(kg/m^2)
     -0.8577     -3.4203     ...      -7.7256     -7.7256
     -0.7478     -3.2195     ...      -7.7256     -7.7256
       .           .         ...        .           .
       .           .         ...        .           .
       .           .         ...        .           .
     -0.0639     -0.1268     ...      -3.2194     -3.4202
     -0.0432     -0.0639     ...      -0.7477     -0.8576
</grid data>

<grid data> | |PM10 Soil Loss|PM10 soil loss|(kg/m^2)
    -0.022817   -0.095288     ...    -0.309679   -0.309679
    -0.019896   -0.089171     ...    -0.309679   -0.309679
       .           .         ...        .           .
       .           .         ...        .           .
       .           .         ...        .           .
    -0.001336   -0.003222     ...    -0.089169   -0.095284
    -0.000663   -0.001336     ...    -0.019894   -0.022815
</grid data>

**Averages - Field
     Total    salt/creep      susp       PM10
     egt                      egtss      egt10
   -----------------kg/m^2--------------------
     -7.9772       -1.9033       -6.0739     -0.232969

**Averages - Crossing Boundaries
Location      Total  Salt/Creep   Susp    PM10
--------------------kg/m----------------------
top       2814.42    671.50   2142.92     82.19
bottom       0.00      0.00      0.00      0.00
right     2814.39    671.50   2142.89     82.19
left         0.00      0.00      0.00      0.00

   Comparision of interior & boundary loss
      interior       boundary    int/bnd ratio
-3971741.0000   3971743.2500          -1.0000

repeat of total, salt/creep, susp, PM10:      7.9772      1.9033      6.0739    0.232969
```

Fig. 30: Example *.egrd file showing, grid parameters, daily total boundary grid emissions and daily total soil loss for each for each grid cell and by component. Grid cells were omitted for brevity and are indicated by ... in both horizontal and vertical

```
 Date of run: Feb 08, 2010 15:02:31
 anemht = 10.00 m    wzoflg = 0
 wind direction = 225.00 deg
 wind direction relative to field orientation = 225.00 deg
 wind quadrant = 6
 orientation and dimensions of sim region
 amasim(deg)  amxsim - (x1,y1) (x2,y2)
     0.00    0.00    0.00  705.61  705.61
 Surface properties
Ridge spacing parallel to wind direction  323.29 (mm)
Crop row spacing 0.20 (mm)
Crop seeding location relative to ridge 0 (0 - furrow, 1 - ridge)
Composite weighted average biomass height 0.76 (m)
Biomass leaf area index 0.00 (m^2/m^2)
Biomass stem area index 0.00 (m^2/m^2)
Biomass flat cover 0.08 (m^2/m^2)
Average yearly total precipitation   300.00 (mm)
 <field dimensions>
       0.00      0.00      0.00    705.61    705.61
 </field dimensions>
 yr mon day hr upd_pd jj nn(subpd) npd (sbqout 1)    1  1  1 15.000   1   1  27 648
 pd wind speed, dir and dir rel to field 27.80 225.00 225.00
 Surface layer properties
Surface course fragments 0.00 (m^3/m^3)
Initial soil mass fraction in surface layer < 0.10 mm  0.15 (kg/kg)
Initial soil mass fraction in surface layer < 0.84 mm  0.48 (kg/kg)
 PM10 emission properties
Soil fraction PM10 in abraded suspension  0.02
Soil fraction PM10 in emitted suspension  0.01
Soil fraction PM10 in saltation breakage suspension  0.05
Coefficient of abrasion of aggregates  0.07
Coefficient of abrasion of crust  0.07
 <grid data> |    1  1  1 15.000|Surface Friction Velocity|friction velocity|(m/s)
 <grid data> |    1  1  1 15.000|Threshold Surface Friction Velocity|threshold friction velocity|(m/s)
 <grid data> |    1  1  1 15.000|Transport Threshold Surface Friction Velocity|transport threshold friction velocity|(m/s)
 <grid data> |    1  1  1 15.000|Surface Random Roughness|random roughness|(mm)
 <grid data> |    1  1  1 15.000|Surface Oriented Roughness|ridge height|(mm)
 <grid data> |    1  1  1 15.000|Surface Rock|surface volume rock fraction|(m^3/m^3)
 <grid data> |    1  1  1 15.000|Soil Agg. Size<0.01|mass fraction < 0.01 mm size|(fract.)
 <grid data> |    1  1  1 15.000|Soil Agg. Size<0.1|mass fraction < 0.1 mm size|(fract.)
 <grid data> |    1  1  1 15.000|Soil Agg. Size<0.84|mass fraction < 0.84 mm size|(fract.)
 <grid data> |    1  1  1 15.000|Soil Agg. Size<2.0|mass fraction < 2.0 mm size|(fract.)
 <grid data> |    1  1  1 15.000|Soil Agg. Size for u* to be the thresh. friction velocity|"effective" mass fraction < 0.84 mm size|
 <grid data> |    1  1  1 15.000|Mobile soil removable from aggregated surface|mass removable|(kg/m^2)
 <grid data> |    1  1  1 15.000|Change in mobile soil on aggregated surface|net mass change|(kg/m^2)
 <grid data> |    1  1  1 15.000|Consolidated crust thickness|crust thickness|(mm)
 <grid data> |    1  1  1 15.000|Fraction of Surface covered with Crust|crust cover|(fract.)
 <grid data> |    1  1  1 15.000|Fraction of Crusted Surface covered with Loose Erodible Soil |loose erodible material|(fract.)
 <grid data> |    1  1  1 15.000|Mass of Loose Erodible Soil on Crusted Surface|loose erodible material|(kg/m^2)
 yr mon day hr upd_pd jj nn(subpd) npd (sbqout 2)    1  1  1 15.037   1   1  27 648
 <grid data> |    1  1  1 15.037|Cumulative Total Soil Loss|soil loss|(kg/m^2)
 <grid data> |    1  1  1 15.037|Cumulative Saltation/Creep Soil Loss|salt/creep soil loss|(kg/m^2)
 <grid data> |    1  1  1 15.037|Cumulative Suspension Soil Loss|suspension soil loss|(kg/m^2)
 <grid data> |    1  1  1 15.037|Cumulative PM10 Soil Loss|PM10 soil loss|(kg/m^2)
 <grid data> |    1  1  1 15.037|Surface Random Roughness (after)|random roughness|(mm)
 <grid data> |    1  1  1 15.037|Surface Oriented Roughness (after)|ridge height|(mm)
 <grid data> |    1  1  1 15.037|Surface Rock (after)|surface volume rock fraction|(m^3/m^3)
 <grid data> |    1  1  1 15.037|Soil Agg. Size < 0.01|mass fraction < 0.01 mm size|(fract.)
 <grid data> |    1  1  1 15.037|Soil Agg. Size < 0.1|mass fraction < 0.1 mm size|(fract.)
 <grid data> |    1  1  1 15.037|Soil Agg. Size < 0.84|mass fraction < 0.84 mm size|(fract.)
 <grid data> |    1  1  1 15.037|Soil Agg. Size < 2.0|mass fraction < 2.0 mm size|(fract.)
 <grid data> |    1  1  1 15.037|Soil Agg. Size for u* to be the thresh. friction velocity (af)|"effective" mass fraction < 0.84 mm s
 <grid data> |    1  1  1 15.037|Mobile soil removable from aggregated surface (after)|mass removable|(kg/m^2)
 <grid data> |    1  1  1 15.037|Change in mobile soil on aggregated surface (after)|net mass change|(kg/m^2)
 <grid data> |    1  1  1 15.037|Consolidated crust thickness (after)|crust thickness|(mm)
 <grid data> |    1  1  1 15.037|Fraction of Surface covered with Crust (after)|crust cover|(fract.)
 <grid data> |    1  1  1 15.037|Fraction of Crusted Surface covered with Loose Erodible Soil(a)|loose erodible material|(fract.)
 <grid data> |    1  1  1 15.037|Mass of Loose Erodible Soil on Crusted Surface (after)|loose erodible material|(kg/m^2)
 egavg =  -0.26 -0.36 -0.41 -0.42 -0.42 -0.42 -0.42 -0.42 -0.42 -0.42 -0.41 -0.41 -0.41 -0.41 -0.41 -0.41 -0.41 -0.41 -0.41 -0.41
 egavg =  -0.41 -0.41 -0.41 -0.41 -0.41 -0.41 -0.41 -0.41 -0.41
 ------------------------------------------------
 yr mon day hr upd_pd jj nn(subpd) npd (sbqout 1)    1  1  1 15.037   2   2  27 648
 pd wind speed, dir and dir rel to field 27.80 225.00 225.00
 Surface layer properties
  ...
 <grid data> |    1  1  1 16.000|Mass of Loose Erodible Soil on Crusted Surface (after)|loose erodible material|(kg/m^2)
 </grid data>
 egavg =  -1.15 -2.66 -4.31 -5.63 -6.48 -6.98 -7.25 -7.42 -7.51 -7.58 -7.63 -7.67 -7.70 -7.73 -7.75 -7.77 -7.79 -7.81 -7.83 -7.85
 egavg =  -7.87 -7.88 -7.90 -7.91 -7.93 -7.94 -7.95 -7.96 -7.98
 ------------------------------------------------
 **Averages - Field
      Total    salt/creep      susp       PM10
      egt                      egtss      egt10
    -----------------kg/m^2--------------------
      -7.9772       -1.9033       -6.0739     -0.232969
 **Averages - Crossing Boundaries
 Location      Total  Salt/Creep   Susp    PM10
 --------------------kg/m----------------------
 top      2814.42    671.50   2142.92     82.19
 bottom      0.00      0.00      0.00      0.00
 right    2814.39    671.50   2142.89     82.19
 left        0.00      0.00      0.00      0.00
    Comparision of interior & boundary loss
       interior       boundary    int/bnd ratio
 -3971741.0000   3971743.2500          -1.0000
```

Fig. 31: Example *.sgrd file showing values presented for each simulation time step. Data values and successive time steps are omitted for brevity. Conditions are given at the beginning of the time step and emissions and conditions upon completion of

References

Allmaras, R. R., R. E. Burwell, W. E. Larson, and R. F. Holt. 1966. "Total porosity and random roughness of the interrow zone as influenced by tillage." USDA Cons. Res. Rep. 7.

Armbrust, D. V., and J. D. Bilbro Jr. 1997. "Relating plant canopy characteristics to soil transport capacity by wind." *Agron. J.* 89:157–162.

Bagnold, R. A. 1943. *The Physics of Blown Sand and Desert Dunes*. London: Methuen.

Chepil, W. S. 1951. "Properties of soil which influence wind eroion. IV. State of dry aggregate structure." *Soil Sci.* 72 (5): 387–401.

Chepil, W. S., and N. P. Woodruff. 1963. "The physics of wind erosion and its control." *Adv. in Agron.* 15:211–302.

Gillette, D. A., D. W. Fryrear, T. E. Gill, T. Ley, T. A. Cahill, and E. A. Gearhart. 1997. "Relation of vertical flux of particles smaller than 10 microns to total aeolian horizontal mass flux at Owens Lake." *J. Geophys. Res.* 102 (D22): 26009–26015.

Greeley, R., and J. D. Iverson. 1985. *Wind as a geological process*. Cambridge England: Cambridge Univ. Press.

Hagen, L. J. 1991a. "A wind erosion prediction system to meet user needs." *J. Soil and Water Conserv.* 46:106–111.

Hagen, L. J. 1996. "Crop residue effects on aerodynamic processes and wind erosion." *Theor. Appl. Climatology* 54:39–46.

Hagen, L. J. 2004. "Fine particulates (PM10 and PM 2.5) Generated by breakage of mobile aggregates during simulated wind erosion." *Trans. ASAE* 47 (1): 107–112.

Hagen, L. J. 2001. "Validation of the Wind Erosion Prediction System (WEPS) erosion submodel on small cropland fields," 479–482. Proc. of International Symposium on Soil Erosion Research For the 21st Century, Jan 3-5, 2001, Honolulu, HI. ASAE.

Hagen, L. J. 1991b. "Wind erosion: Emission rates and transport capacities on rough surfaces." ASAE paper no. 912082. St. Joseph, MI.

Hagen, L. J. 1991c. "Wind erosion mechanics: Abrasion of aggregated soil." *Trans. ASAE (Corrected)* 34 (4): 831–837.

Hagen, L. J., and D. V. Armbrust. 1992. "Aerodynamic roughness and saltation trapping efficiency of tillage ridges." *Trans. ASAE* 35 (4): 1179–1184.

Hagen, L. J., and D. V. Armbrust. 1994. "Plant canopy effects on wind erosion saltation." *Trans. ASAE* 37 (2): 461–465.

Hagen, L. J., N. Mirzamostafa, and A. Hawkins. 1996. "PM-10 generation by wind erosion," 76–86. International Conference on Air Pollution from Agricultural Operations, February 7-9, 1996, Kansas City, MO. Ames, IA: MidWest Plan Service.

Hagen, L. J., E. L. Skidmore, P. L. Miller, and J. E. Kipp. 1981. "Simulation of the effect of wind barriers on airflow." 24 (4): 1002–1008.

Hagen, L. J., E. L. Skidmore, and A. Saleh. 1992. "Prediction of aggregate abrasion coefficients." *Trans. ASAE* 35 (6): 1847–1850.

Hagen, L. J., S. van Pelt, T. M. Zobeck, and A. Retta. 2007. "Dust deposition near an eroding source field. Earth Surface Processes and Landforms." 32 (2): 281–289.

Hagen, L. J., L. E. Wagner, J. Tatarko, E. L. Skidmore, A. A. Durar, J. L. Steiner, H. H. Schomberg, A. Retta, D. V. Armbrust, T. M. Zobeck, P. W. Unger, D. Ding, and I. Elminyawi. 1995. "USDA Wind Erosion Prediction System: Technical description," 9–11. Proc. of WEPP/WEPS Symposium, August 9-11, Des Moines, IA. Ankeny, IA: Soil / Water Conservation Society.

Hiesler, G. M., and D. R. DeWalle. 1988. "Effects of Windbreak Structure on Wind Flow." *Agriculture, Ecosystems and Environment* 22:41–69.

Lettau, H. H., and K. Lettau. 1978. "Experimental and micro-meteorological studies of dune migration." In *Exploring the World's Driest Climate*, ed. by H. H. Lettau and K. Lettau, 110–147. Madison, Wisconsin: Institute of Environmental Studies, University of Wisconsin.

Lyles, L., and B. E. Allision. 1976. "Wind erosion: The protective role of simulated standing stubble." *Trans. ASAE* 19 (1): 61–64.

Mirzamostafa, N. 1996. "Suspension component of wind erosion." PhD thesis, Kansas State University.

Mirzamostafa, N., L. J. Hagen, L. R. Stone, and E. L. Skidmore. 1998. "Soil aggregate and texture effects on suspension components from wind erosion." *Soil Sci. Soc. Am. J.* 62 (5): 1351–1361.

Panofsky, H. A., and J. A. Dutton. 1984. *Atmospheric turbulence*. 397. New York: John Wiley & Sons.

Potter, K. N., and T. M. Zobeck. 1990. "Estimation of soil microrelief." *Trans. ASAE* 33 (1): 156–161.

Potter, K. N., T. M. Zobeck, and L. J. Hagen. 1990. "A microrelief index to estimate soil erodibility by wind." *Trans. ASAE* 33 (1): 151–155.

Priestley, C. H. B. 1959. *Turbulent Transfer in the Lower Atmosphere*. Chicago, Illinois, U.S.A.: The University of Chicago Press.

Pye, K. 1987. *Aeolian dust and dust deposits*. London: Academic Press.

Raine, J. K., and D. C. Stevenson. 1977. "Wind protection by model fences in a simulated atmospheric boundary layer." *Journal of Industrial Aerodynamics* 2:159–180.

Raupach, M. R. 1992. "Drag and drag partition on rough surfaces." *Boundary Layer Meteorol.* 60:375–395.

Saleh, A., and D. W. Fryrear. 1995. "Threshold wind velocities of wet soils as affected by wind blown sand." *Soil Sci.* 160 (4): 304–309.

Stout, J. 1990. "Wind erosion within a simple field." *Trans. ASAE* 33 (5): 1597–1600.

USDA-ARS. 2013. "WEPS - Researcher, Developer, Public Release." Accessed 28 March 2016, no. 1.3.9. `http://www.ars.usda.gov/services/software/download.htm?softwareid=415`.

Van de Ven, T. A. M., D. W. Fryrear, and W. P. Spaan. 1989. "Vegetation characteristics and soil loss by wind." *J. Soil and Water Conserv.* 44:347–349.

Van Donk, S. J., L. E. Wagner, E. L. Skidmore, and J. Tatarko. 2005. "Comparison of the Weibull Model with Measured Wind Speed Distributions for Stochastic Wind Generation." *Trans. ASAE* 48 (2): 503–510.

Van Eimern, J., R. Karschon, L. A. Razumova, and G. W. Roberston. 1964. "Windbreaks and shelterbelts," 188. World Meteorol. Organ. Tech. Notes 59.

Vigiak, O., G. Sterk, A. Warren, and L. J. Hagen. 2003. "Spatial modeling of wind speed around windbreaks." *Catena* 52:273–288.

Wagner, L. E., and D. Ding. 1994. "Representing aggregate size distribution as modified lognormal distributions." *Trans. ASAE* 37 (3): 815–821.

Zobeck, T. M., and D. W. Fryrear. 1986. "Chemical and physical characteristics of windblown sediment, I. Quantities and physical characteristics." *Trans. ASAE* 29 (4): 1032–1036.

Zobeck, T. M., and T. W. Popham. 1991. "Influence of abrader flux and soil properties." *Soil Sci. Am. J.* 55 (4): 1091–1097.

8 Symbols and Definitions

Symbol	Definition	Units	Variable Name
a,c	distances from the grid cell to the barrier ends	m	a,c
aa,ca	angles at the barrier ends	$degrees$	aa,ca
$alpha$,$ceta$	angles from the line passing through the cell coordinates toward the positive y axis direction and lines a and$c$	$degrees$	alpha, ceta
awa	wind direction relative to the simulation region y-axis	$degrees$	awa
$awar_k$	cardinal wind direction k relative to the simulation region y-axis	$degrees$	awar(k)
$amasim$	angle of the simulation region y-axis relative to geographic north	$degrees$	amasim
b	barrier length	m	b
$b1$,$b2$	coefficients used in Eq. 70		b1,b2
$b1^{ic}$,$b2^{ic}$	coefficients for smooth surface (aerodynamic roughness equals 0.5mm)		b1,b2
BD_{lai}	decomposing biomass leaf area index	$\frac{m^2}{m^2}$	bdrlai
BD_{sai}	decomposing biomass stem area index	$\left(\frac{m^2}{m^2}\right)$	bdrsai
BFF_{cv}	biomass fraction of flat cover		bffcv
BR_{cd}	effective biomass drag coefficient		brcd
BR_{lai}	biomass effective leaf area index	$\frac{m^2}{m^2}$	bbrlai
BR_{sai}	biomass effective stem area index	$\frac{m^2}{m^2}$	bbrsai
BZ	biomass height	m	abzht
$C10_{dp}$	coefficient of deposition for PM_{10}, estimated as 0.001	$\frac{1}{m}$	c10dp
C_{an_i}	coefficient of abrasion for aggregates and crust (C_{an_1}=C_{anag},C_{an_2}=C_{ancr})	$\frac{1}{m}$	
C_{anag}	abrasion coefficient for aggregates	$\frac{1}{m}$	canag

Symbol	Definition	Units	Variable Name
C_{ancr}	abrasion coefficient for crust	$\frac{1}{m}$	cancr
C_{bk}	coefficient of breakage	$\frac{1}{m}$	cbk
C_{dp}	coefficient of deposition of suspension-size	$\frac{1}{m}$	cdp
C_{en}	coefficient of emission	$\frac{1}{m}$	cen
C_{eno}	coefficient of emission for a bare, smooth, loose, erodible soil. A typical field value is about 0.06	$\frac{1}{m}$	ceno
C_i	coefficient of plant interception	$\frac{1}{m}$	ci
C_{lai}	growing crop leaf area index	$\frac{m^2}{m^2}$	bcrlai
C_m	a coefficient of mixing, value about$(0.0001\, SFss_{en})$	$\frac{1}{m}$	cm
CR_{los}	roughness dependent fraction of mobile crust cover reduction coefficient		crlos
C_s	the saltation transport parameter, with a typical value of about 0.3 or for surfaces armored with stones a greater value	$\frac{kg \bullet s^2}{m^4}$	cs
C_{sai}	growing crop stem area index	$\frac{m^2}{m^2}$	bcrsai
Css_i	fraction of suspension-size aggregate flux intercepted by standing biomass		
C_t	coefficient of surface trapping	$\frac{1}{m}$	ct
C_{tf}	empirical coefficient, with value about 1.2		ctf
CX_{row}	growing crop row spacing	m	bcxrow
CZ	growing crop height	m	bczht
d_{min}	minimum distance between the cell center and the barrier	m	dmin
$\triangle t$	surface update time interval	s	time
$\triangle X$	effective distance wind travels across grid cell	m	lx
dm_{los}	cumulative mobile soil loss or gain on aggregated surface	$\frac{kg}{m^2}$	dmlos
dm_{los0}	value of dm_{los} at prior time step	$\frac{kg}{m^2}$	
dmt	net gain(+) or loss(-) of soil from grid in time interval $\triangle t$	$\frac{kg}{m^2}$	dmt
dmt_{los}	net change in mobile soil surface aggregates during time interval $\triangle t$	$\frac{kg}{m^2}$	dmtlos
ENG_e	relative erosive wind energy	$\frac{m^3}{s^3}$	enge
F_{an_i}	mass fraction saltation impacting immobile aggregates and unprotected surface crust (F_{an_1}=F_{anag},F_{an_2}=F_{ancr})		
F_{anag}	fraction of saltation/creep impacting immobile aggregates		fanag
F_{ancr}	fraction of saltation/creep impacting on unprotected surface crust		fancr

Symbol	Definition	Units	Variable Name
fdm	additional net change in mobile soil surface aggregates for aggregated surface during time interval $\triangle t$	$\frac{kg}{m^2}$	fdm
fu_*	fraction of open field friction velocity		fu
$fu_*^{i,j,k}$	the reduction in wind velocity due to barriers for cell i,j from the wind direction k		w0br(i,j,k)
G_{an}	vertical flux from abrasion of surface clods and crust	$\frac{kg}{m^2 s}$	
G_{en}	vertical flux from emission of loose aggregates	$\frac{kg}{m^2 s}$	
Gss_{an}	vertical flux of suspension-size aggregates created by abrasion of clods and crust	$\frac{kg}{m^2 s}$	
Gss_{bk}	vertical flux of suspension-size aggregates created by breakage of saltation/creep-size aggregates	$\frac{kg}{m^2 s}$	
Gss_{dp}	vertical flux (deposition) of suspension-size aggregates above a non-eroding surface	$\frac{kg}{m^2 s}$	
Gss_{en}	vertical emission flux of loose, suspension-size aggregates	$\frac{kg}{m^2 s}$	
G_{tp}	vertical flux from trapping of saltation/creep aggregates	$\frac{kg}{m^2 s}$	
hl	ridge height divided by ridge spacing		hl
$HR0_{wc}$	surface soil water content	$\frac{kg}{kg}$	hrwc0
$HR15_{wc}$	surface soil water content at 1.5 MPa	$\frac{kg}{kg}$	hrwcw
ix	grid cell spacing in the x direction	m	ix
jy	grid cell spacing in the y direction	m	jy
k	index of cardinal wind directions in clockwise direction (k=1 is north)		
K	Von Karmen's constant (approximately equal to 0.4)		
m, n, s, t	barrier friction velocity reduction equation coefficients		m, n, s, t
N	number of time steps for surface updating for each wind speed interval		n
N_t	minimum number of time steps required for surface updating for each wind speed interval		n
N_{tstep}	number of wind speed intervals input in 24 hour time period		ntstep
pb	effective barrier porosity		pb
pbr	optical barrier porosity		pbr

Symbol	Definition	Units	Variable Name
$q10_1$	grid cell incoming PM_{10}	$\frac{kg}{m \cdot s}$	q10i
q_1	grid cell incoming saltation/creep	$\frac{kg}{m \cdot s}$	qi
q_{cp}	transport capacity of the surface	$\frac{kg}{m \cdot s}$	qcp
q_{en}	transport capacity	$\frac{kg}{m \cdot s}$	qen
q_s	discharge of primary (non-breakable) sand particles	$\frac{kg}{m \cdot s}$	
q_{sc}	horizontal saltation/creep discharge	$\frac{kg}{m \cdot s}$	qo
q_{ss}	horizontal suspension component discharge	$\frac{kg}{m \cdot s}$	
qss_o	maximum value of q_{ss} entering deposition region	$\frac{kg}{m \cdot s}$	
q_{ss1}	grid cell incoming suspension	$\frac{kg}{m \cdot s}$	qssi
q_{ss2}	suspension discharge at downwind location X_2	$\frac{kg}{m \cdot s}$	qsso
R_{crow}	reduction of effective leaf area when crop rows spaced >5 crop heights		red_fac
R_{enb}	bare soil emission ratio accounting for immobile cover and surface roughness		renb
R_{env}	emission ratio accounting for flat, random vegetation		renv
R_{rg}	reduction of effective leaf and stem area when crop partly sheltered in furrow		red_fac
rut	ratio of friction velocity for this time period to daily initial threshold friction velocity		rut
SAC_{rg}	Weibull scale factor for ridge shelter	$degrees$	sargc
SAC_{rr}	Weibull scale factor for random roughness	$degrees$	sarrc
SAI	stem silhouette area index		bcrsai
SD_{agd}	aggregate density	$\frac{Mg}{m^3}$	sdagd
SE_{ags}	dry stability of immobile aggregates	$\ln\left(\frac{J}{kg}\right)$	seags
SE_{crs}	dry stability of crust	$\ln\left(\frac{J}{kg}\right)$	secr
$SF10_{an}$	soil fraction of PM_{10} in suspension-size aggregates created during abrasion of clods and crust		sf10an
$SF10_{bk}$	soil fraction of PM_{10} in suspension-size aggregates broken from saltation and creep-size aggregates		sf10bk
$SF10_{en}$	soil fraction of PM_{10} in suspension-size surface soil		sf10en
SF_{10}	soil fraction less than 0.10 mm diameter		sf10
SF_{10ic}	is the SF_{10} initial condition at the beginning of the erosion event		sf10ic

Symbol	Definition	Units	Variable Name
SF_{200}	soil fraction less than 2.0 mm diameter		sf200
SF_{84}	soil fraction covered with aggregates <0.84 mm in diameter on the non-crusted area, but excluding the fraction of rock-covered area		sf84
SF_{84ic}	is the SF_{84} initial condition at the beginning of the erosion event		sf84ic
SF_{84mn}	minimum mobile soil fraction for emission		sf84mn
SFA_{12}	total fraction of area sheltered with shelter angles >12 degrees		sfa12
SFA_{12rg}	surface fraction of area with shelter angles >12 degrees for ridges		
SFA_{12rr}	surface fraction of area with shelter angles >12 degrees for random roughness		
SF_{cla}	surface soil fraction clay		sfcla
SF_{cr}	soil fraction covered by crust, but excluding the fraction of rock-covered area		sfcr
SF_{cr0}	crust cover fraction at prior time step		
SF_{cv}	soil fraction covered by clod, crust, and rock so it does not emit		sfcv
SF_{cv}^{ic}	bare surface cover fraction before erosion occurs ($SF_{84}^{ic} = SF_{84}$before erosion begins)		
SF_{cv}^{lim}	soil fraction limited by ability of friction velocity to move soil particles		
$SFer$	soil mass fraction of loose, erodible-size, less than about 2.0 mm		
SF_{los}	soil fraction covered with loose, erodible soil on the crusted area		sflos
SF_{san}	surface soil fraction sand		sfsan
SF_{sil}	surface soil fraction silt		sfsil
$SFss$	soil mass fraction of loose, suspension-size less than about 0.1 mm		
$SFss_{an}$	mass fraction of suspension-size from abrasion		sfssan
$SFss_{en}$	mass fraction of suspension-size ($< 0.10\,mm$) among loose aggregates ($< 2.0\,mm$ diameter)		sfssen
SF_{vfs}	surface soil fraction very fine sand		sfvfs
SL_{agn}	lower limit of size distribution	mm	slagn
SL_{agx}	upper limit of size distribution	mm	slagx
SL_{agm}	geometric mean of size distribution	mm	slagm
SM_{aglos}	mass of mobile soil particles	$\frac{kg}{m^2}$	smaglos

Symbol	Definition	Units	Variable Name
$SM_{aglosmx}$	mass of mobile soil particles for a bare smooth surface at a friction velocity of 0.75 $\frac{m}{s}$	$\frac{kg}{m^2}$	sma-glosmx
SM_{los}	mobile soil aggregates per unit area of the crusted surface	$\frac{kg}{m^2}$	smlos
SM_{los0}	value of SM_{los}at prior time step	$\frac{kg}{m^2}$	
SO_{ags}	geometric standard deviation of size distribution	mm	s0ags
SV_{roc}	soil volume rock >2.0 mm	$\frac{m^3}{m^3}$	svroc
SV_{roc0}	soil rock volume at prior time-step	$\frac{m^3}{m^3}$	
SV_{rocic}	soil rock volume at beginning of erosion event	$\frac{m^3}{m^3}$	
SX_{dk}	furrow dike spacing	mm	asxdks
SX_{rg}	ridge spacing	mm	asxrgs
SA_{rg}	ridge orientation, clockwise from north and parallel to the ridge	$degrees$	asargo
SXP_{rg}	ridge spacing parallel the wind direction	mm	sxprg
SZ_{an}	change is roughness height caused by abrasion for time step $\triangle t$	mm	
SZ_{cr}	crust thickness	mm	szcr
SZ_{cr0}	crust thickness at prior time step	mm	
SZ_{rg}	ridge height	mm	szrgh
SZ_{rg0}	ridge height at prior time-step	mm	
SZ_{rr}	random roughness	mm	slrr
SZ_{rr0}	random roughness at prior time-step	mm	
SZ_t	total change is roughness height for time step $\triangle t$	mm	
SZ_v	change is roughness height caused by deposition or emission for time step $\triangle t$	mm	szv
U	wind velocity at height Z	$\frac{m}{s}$	
U_{st}	wind speed at weather station	$\frac{m}{s}$	awu
U_*	friction velocity	$\frac{m}{s}$	wus
U_*	friction velocity at soil surface below standing biomass	$\frac{m}{s}$	
$U_*^{i,j}$	the adjusted friction velocity for cell i, j with wind from direction k	$\frac{m}{s}$	wus(i,j)
U_{*e}	estimated friction velocity found to be 0.06 of the 10 meter wind velocity for this time period	$\frac{m}{s}$	wuse
U_{*st}	friction velocity at the weather station	$\frac{m}{s}$	wusst
U_{*t}	dynamic threshold friction velocity	$\frac{m}{s}$	
U_{*te}	estimated threshold friction velocity found to be $\frac{U_{*e}}{rut}$	$\frac{m}{s}$	wuste

Symbol	Definition	Units	Variable Name
U_{*to}	threshold friction velocity of a bare smooth surface with the erodible fraction of the surface before erosion occurs	$\frac{m}{s}$	wusto
U_{*tp}	static threshold friction velocity for trapping and transport capacity	$\frac{m}{s}$	wusp
U_{*ts}	adjusted surface static threshold friction velocity	$\frac{m}{s}$	wust
U_{*tt}	dynamic threshold friction velocity of bare surface	$\frac{m}{s}$	
U_{*v}	friction velocity above the surface including any standing biomass	$\frac{m}{s}$	wusv
UB_{*ts}	static threshold friction velocity of bare surface	$\frac{m}{s}$	wubsts
UC_{*ts}	change in static threshold friction velocity caused by flat biomass cover	$\frac{m}{s}$	wucsts
UD_{*ts}	change in static threshold friction velocity from variable aggregate density	$\frac{m}{s}$	wucdts
UW_{*ts}	increase in static threshold friction velocity from surface wetness	$\frac{m}{s}$	wucwts
w	distance between the barrier and the grid cell along the wind direction vector	m	w
waa	angle between the barrier and the wind direction	$degrees$	waa
WA_{dir}	wind direction relative to geographic north	$degrees$	awadir
wz	distance from barrier w converted to units of barrier heights		x
WZ_{ypt}	average annual precipitation	mm	awzypt
X	downwind distance from nonerodible boundary	m	
x_i,y_j	coordinates of the center of each cell	m	lx, ly
xbr	normalized barrier width (barrier width divided by barrier height)		xw
$Z0$	aerodynamic roughness length	mm	sbz0
$Z0_{rg}$	aerodynamic roughness of the ridges	mm	wzorg
$Z0_{rr}$	aerodynamic roughness of random roughness including any flat biomass cover	mm	wzorr
$Z0_{st}$	aerodynamic roughness at weather station, assumed to be 25 mm in WEPS	mm	awzzo
Z	height above the surface	mm	
Z_d	zero-plane displacement	mm	

Symbol	Definition	Units	Variable Name
Z_{st}	anemometer height at the weather station; (wind speeds were adjusted to 10 m height in WEPS data base)	mm	anemht
$Z0_v$	as defined by Eq. 49, 50, and 51	mm	wzzov